Ore Geology Reviews 78 (2016) 424–446

Contents lists available at ScienceDirect

Ore Geology Reviews

journal homepage: www.elsevier.com/locate/oregeorev

Transpressional imbricate thrust zones controlling gold mineralization in the Central Eastern Desert of Egypt

Mohamed A. Abd El-Wahed [a,*], Hassan Harraz [a], Mohamed H. El-Behairy [b]

[a] Geology Department, Faculty of Science, Tanta University, Tanta 31527, Egypt
[b] Centamin Egypt Ltd, 361 El-Horreya Road, Sedi Gaber, Alexandria, Egypt

ARTICLE INFO

Article history:
Received 31 October 2015
Received in revised form 26 March 2016
Accepted 30 March 2016
Available online 9 April 2016

Keywords:
Transpression
Sukari gold mine area
Central Eastern Desert
Imbricate thrust
Thrust duplex

ABSTRACT

Strongly deformed volcaniclastic metasediments and ophiolitic slices hosting the Sukari gold mineralization display evidence of a complex structural evolution involving three main ductile deformational events (D_1–D_3). D_1 produced ENE-trending folds associated with NNW-propagating thrust slices and intrusion of the Sukari granite (689 ± 3 Ma). D_2 formed a moderately to steeply dipping, NNW-trending S_2 foliation curved to NE and developed arcuate structure constituting the Kurdeman shear zone (≤595 Ma) and East Sukari imbricate thrust belt. Major NE-trending F_2 folds, NW-dipping high-angle thrusts, shallow and steeply plunging mineral lineation and shear indicators recorded both subhorizontal and subvertical transport direction during D_2. D_3 (560–540 Ma) formed NNE-trending S_3 crenulation cleavage, tight F_3 folds, Sukari Thrust and West Sukari imbricate thrust. The system of NW-trending sinistral Kurdeman shear zone (lateral ramps and tear faults) and imbricate thrusts (frontal ramps) forming the actuate structure developed during SE-directed thrusting, whereas the prevailing pattern of NNE-trending dextral Sukari shear zone and imbricate thrusts forming Sukari thrust duplex developed during NE-directed tectonic shearing. Sukari granite intruded in different pluses between 689 and 540 Ma and associated with at least four phases of quartz veins with different geometry and orientation. Structural analysis of the shear fabrics indicates that the geometry of the mineralized quartz veins and alteration patterns are controlled by the regional NNW- and NE-trending conjugate zones of transpression. Gold-bearing quartz veins are located within NNW-oriented sinistral shear zones in Kurdeman gold mine area, within steeply dipping NW- and SE dipping thrusts and NE- and NS-oriented dextral and sinistral shear zones around Sukari mine area, and along E-dipping backthrusts and NW-SE and N-S fractures in Sukari granite. The high grade of gold mineralization in Sukari is mainly controlled by SE-dipping back-thrusts branched from the major NW-dipping Sukari Thrust. The gold mineralization in Sukari gold mine and neighboring areas in the Central Eastern Desert of Egypt is mainly controlled by the conjugate shear zones of the Najd Fault System and related to E-W directed shortening associated with oblique convergence between East and West Gondwana.

1. Introduction

The Eastern Desert of Egypt represents the northwestern continuation of the Arabian Nubian Shield (ANS), which lies within the suture between East and West Gondwana (Fig. 1) at the northern end of the Neoproterozoic East African Orogen (EAO). The ANS formed during Cryogenian–Ediacaran time (790–560 Ma) and was generated in association with the breakup of Rodinia ~800–900 Ma and closure of the Mozambique Ocean (Stern et al., 2004) due to collision between East and West Gondwanaland at ~600 Ma.

The Eastern Desert of Egypt represents the northwestern continuation of the ANS which developed as crust of Middle Cryogenian–Ediacaran age (790–560 Ma) between northeast Africa and west Arabia (Fig. 1). This crust is the northern extension of the EAO and was generated in association with the ~800–900 Ma breakup of Rodinia and closing of the Mozambique Ocean (Stern et al., 2004) due to collision between East and West Gondwanaland at ~600 Ma (Meert, 2003; Fritz et al., 2013). The EAO is an extensive Neoproterozoic accretionary orogen and collisional zone within Gondwana (Stern, 1994; Johnson et al., 2011). The late Proterozoic Arabian–Nubian Shield (ANS) forms the suture between East and West Gondwana at the northern end of the East African Orogen.

The tectonic evolution of the Arabian–Nubian Shield encompasses three stages spread over 600 Ma: accumulation of arc terrains within the Hijaz Magmatic Arc, followed by accretion of the Hijaz Magmatic Arc against the Nile Craton (Fig. 1), and post-accretion reworking of the accreted arc (Camp, 1984; Abdelsalam and Stern, 1996; Fritz et al., 1996; Augland et al., 2012).

The Central Eastern Desert (CED) is occupied by two main tectonostratigraphic units: (1) the structural unit (gneisses, migmatites, schists and amphibolites) and (2) Pan-African nappes including

* Corresponding author.
E-mail address: mohamed.abdelwahad@science.tanta.edu.eg (M.A. Abd El-Wahed).

http://dx.doi.org/10.1016/j.oregeorev.2016.03.022
0169-1368/

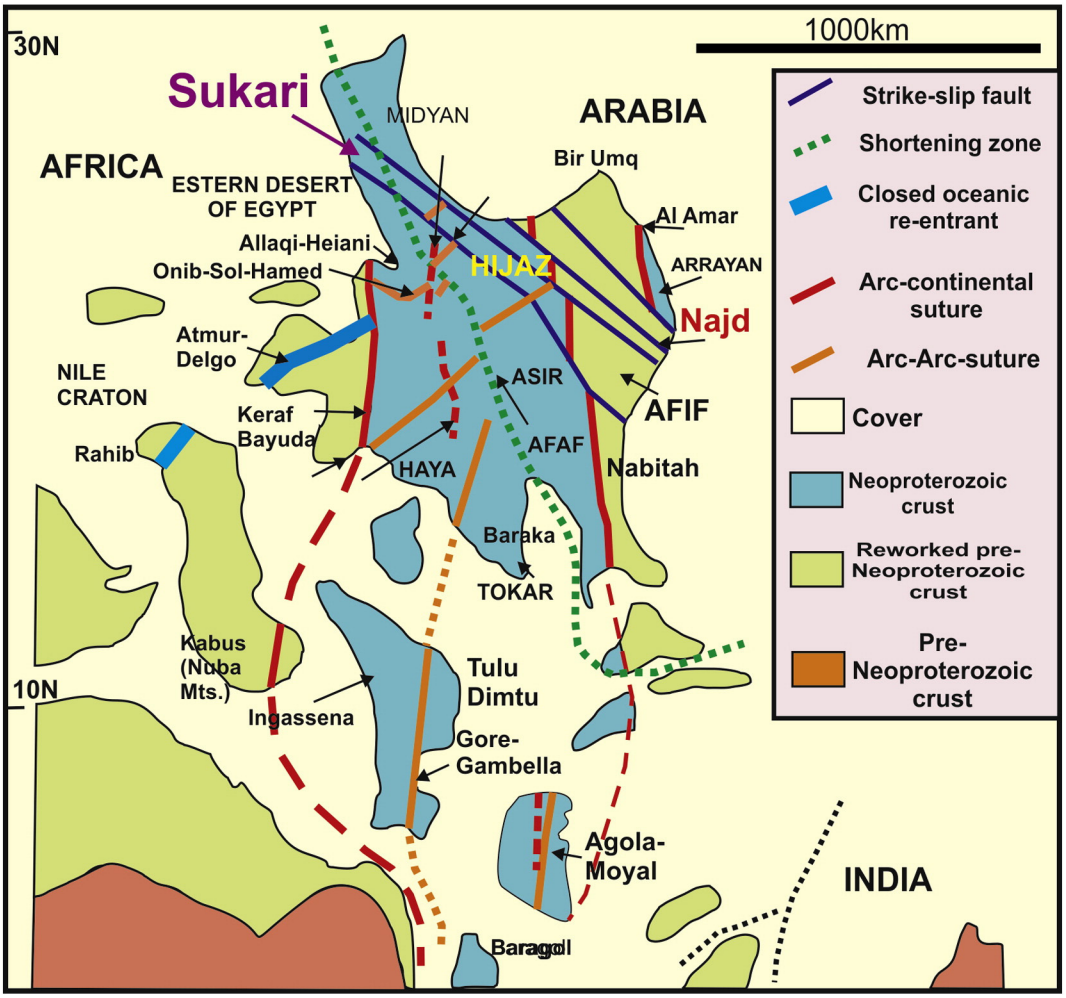

Fig. 1. Tectonic map of the Arabian–Nubian Shield (ANS) showing the location of Sukari relative to the Hijaz Magmatic Arc and the Nile Craton (after Abdelsalam and Stern, 1996).

low grade metamorphosed ophiolite slices (serpentinites, pillow lavas and metagabbros), arc metavolcanics, and arc metasediments. These two units were intruded by syn-tectonic calc-alkaline granites and metagabbro–diorite complex (606–614 Ma) and then by late to post-tectonic granites at ~590–550 Ma (Rice et al., 1993; Andresen et al., 2010).

The ultramafic rocks associated with ANS ophiolites are largely converted to serpentinite or to mixtures of serpentine, talc, tremolite, magnesite, chlorite, magnetite, and carbonate (talc-carbonate schists or listwaenite) (Stern et al., 2004; Abu-Alam and Hamdy, 2014). There is a direct relationship between carbonatization of ultramafic rocks, subsequent granite intrusions, and gold and talc mineralization. Carbonatization has resulted in gold concentrations up to a thousand times that of the original ultramafic rocks (Buisson and Leblanc, 1987; Azer, 2013).

The CED of Egypt is marked by prevalence of a NW-trending structural fabrics (Fig. 2) and the presence of structural windows (e.g. Hafafit, Sibai and Meatiq core complexes) that developed during sinistral movement along the NW-SE trending shear zone within the Najd Fault System (NFS) (Fritz et al., 1996; Abd El-Wahed, 2008, 2010). The NFS is a complex set of left-lateral strike-slip faults and ductile shear zones that strike NW-SE across the ANS (Stern, 1985). The central part of the CED is further characterized by prominent NE-, ENE- and E-W-trending tectonic fabrics developed along NE-trending, dextral strike-slip shear zones (Shalaby et al., 2005; Abd El-Wahed and Kamh, 2010; Abd El-Wahed, 2014; Abdeen et al., 2014).

The NW-trending sinistral strike-slip shear zones define the northeast and southwest borders of the core complexes (e.g. Hafafit, Sibai and Meatiq, see Fig. 2), such as the Nugrus shear zone to the east of Hafafit metamorphic core complex and to the west of the map area. This shear zone was previously interpreted as a thrust (Fig. 2) (Nugrus Thrust, Greiling et al., 1988) separating the Hafafit metamorphic core complex (footwall) and the Pan-African nappes of the Wadi Ghadir mélange. It was later interpreted as a left-lateral ductile shear zone dominated by strike-slip duplexes and linked with imbricate ramps and thrusts (Nugrus Fault, Fritz et al., 1996; Unzog and Kurz, 2000; Helmy et al., 2004; Shalaby et al., 2005). Subsequently, Fowler and Osman (2009) considered Nugrus shear zone as a post-arc collision low-angle normal ductile shear zone formed during the Neoproterozoic extensional tectonic phase. Lundmark et al. (2012) assigned an age of ≤595 Ma for left-lateral shearing of the Nugrus Shear Zone. The NW-trending thrusts east of the Hafafit core complex (Wadi Ghadir mélange) are deflected into NE-SW trends around the Sukari gold mine and thus define an example of a flower structure related to sinistral transpression along the Nugrus shear zone (Fritz et al., 1996; Shalaby et al., 2005). Some authors had previously mapped these NE-trending thrusts as SE-dipping (e.g. Fritz et al., 1996, 2002), it is clearly demonstrable that they dip towards the NW (Akaad et al., 1993; Abd El-Wahed and Kamh, 2010; Abd El-Wahed, 2014).

The Sukari gold mine is the first large-scale modern gold mine in Egypt. It is located in the Central Eastern Desert of Egypt, about 30 km southwest of the Red Sea coastal town of Marsa Alam and to the northeast of Hafafit core complex (Fig. 2). It lies within an arcuate structure which is trending NW-SE in the south and NE-SW in the north. Detailed mapping, geochemical exploration and drilling were carried out in the Sukari gold mine area by Centamin Egypt Ltd.

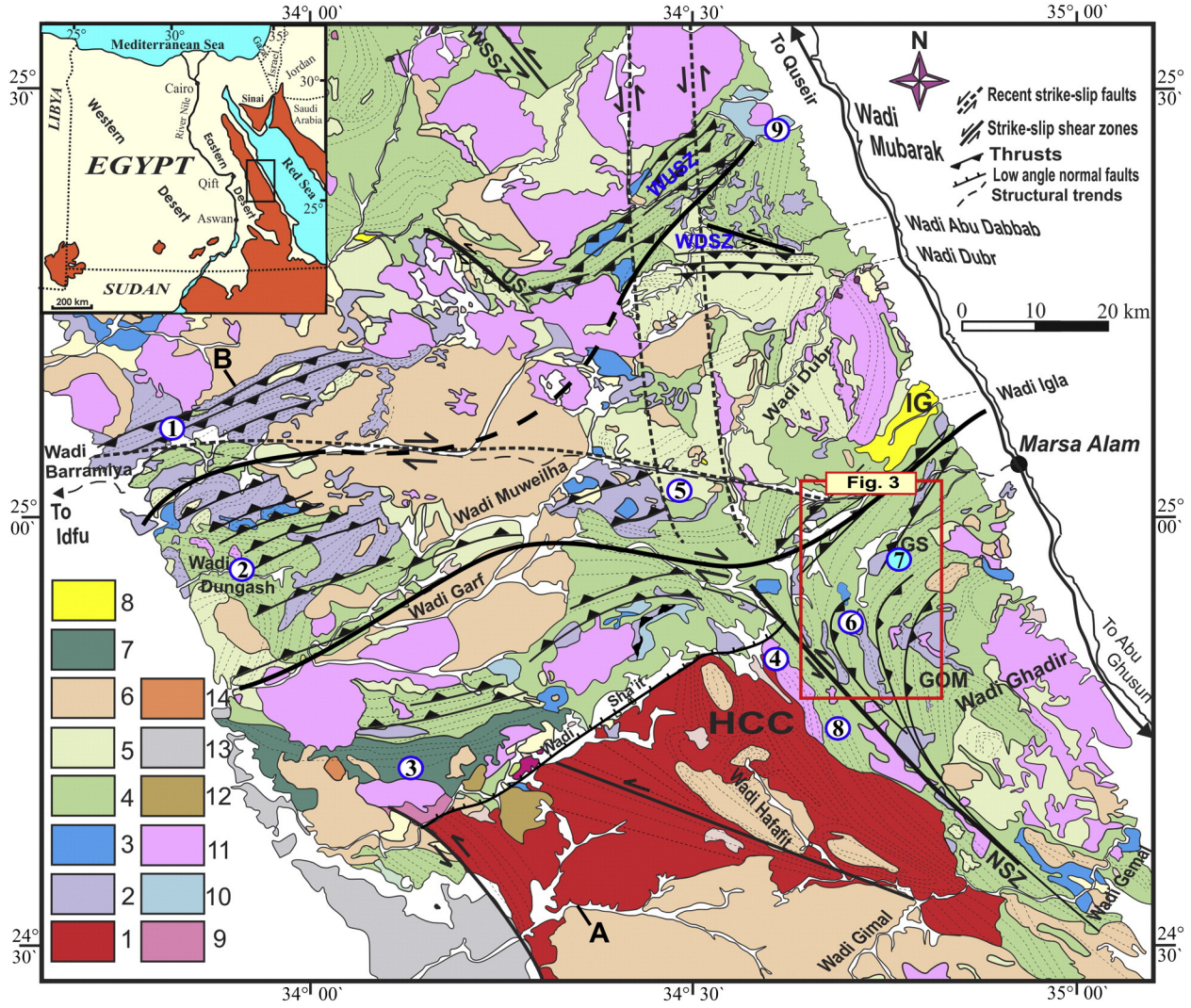

Fig. 2. Geological map of the southern part of the Central Eastern Desert of Egypt (modified after Abd El-Wahed (2014)). 1; core complexes 2; serpentinites, 3; ophiolitic metagabbros, 4; metavolcanics and metasediments, 5; syn-tectonic intrusive metagabbros, 6; syn-tectonic granite, 7; Dokhan volcanics, 8; molasse sediments, 9; felsites, 10; gabbros, 11; post to late tectonic granites; 12; ring complex, 13; Natash volcanics and 14; trachyte plugs. HCC; Hafafit core complex, GOM; Wadi Ghadir ophiolitic mèlange, NSZ; Wadi Nugrus shear zone, WDSZ; Wadi Abu Dabbab shear zone, WUSZ; Wadi El Umra shear zone, GS; Gabal Sukari and Sukari gold mine, IG; Igla molasse basin, USZ; Um Nar shear zone, WSSZ; Wadi Sitra shear zone. Gold mines in the Central Eastern Desert: 1; Barramiya, 2; Dungash, 3; Hamash, 4; Hangalia, 5; Atud, 6; Kurdeman, 7; Sukari, 8; Um Ud, 9; Um Rus.

Sukari produced 377,261 oz of gold in 2014. The total measured and indicated resource, at 30 June 2015, was 13 million ounces (Moz) gold and the open pit mineral reserve is reported as an open pit resource at 0.3 g/t cut-off grade. The total combined open pit and underground reserve estimate, at 30 June 2015, was 8.3 Moz (http://www.centamin.com), making Sukari the most significant gold deposits in Egypt.

The primary aim of this study is to understand how differing styles of Au mineralization developed along the two dominant structural trends (NW- and NE-trending tectonic fabrics) around the Sukari gold mine area. A secondary aim is to provide a comprehensive structural description of the Sukari gold mine area and draw conclusions about: (1) the relation between dextral and sinistral transpressive shear zones; (2) the NE-striking thrusts with two opposing dip directions; (3) the nature and distribution of gold-bearing quartz veins along the two trends.

The Au contents used in this study were obtained from Centamin Egypt Ltd. The Au contents were determined by using aqua-regia solutions (AR) and Fire Assay (FA) using Lead collection. Perkin Elmer Optima 8300 and Thermo Fisher iCAP 6000 Series instruments for the fire assay analysis. Analyses were done by Bureau Veritas Australia Pty Ltd. with lower Detection limits is 0.0005 ppm.

2. Geology of the Sukari area

The Sukari gold mine area is dominated by mafic–ultramafic ophiolitic rocks, island arc-related volcaniclastic metasediments-plutonic assemblages, and syn-orogonic intrusions. All these rocks are cut later by dolerite, diorite and felsic dykes (Fig. 3).

The ophiolitic suite in the Sukari area is dismembered and comprises serpentinite–talc–carbonate and metagabbro–diorite complexes. This ophiolitic suite is overlain by volcaniclastic metasediments deposited within an island arc setting and then intruded by Sukari granites. The original distribution of stratigraphic units has been disrupted. The serpentinites and talc carbonate rocks occur as scattered bodies within the predominantly metavolcanic and metapyroclastic island arc assemblages. The contacts between the serpentinite–talc–carbonate rocks and the enclosing country rocks are tectonic, whereas the contacts between serpentinite–talc–carbonate rocks and metagabbro–diorite are gradational.

The volcaniclastic metasediments are the most widely distributed rock units in the present area. This unit forms an elongate belt trending NE-SW and is composed essentially of very thick and widespread mature

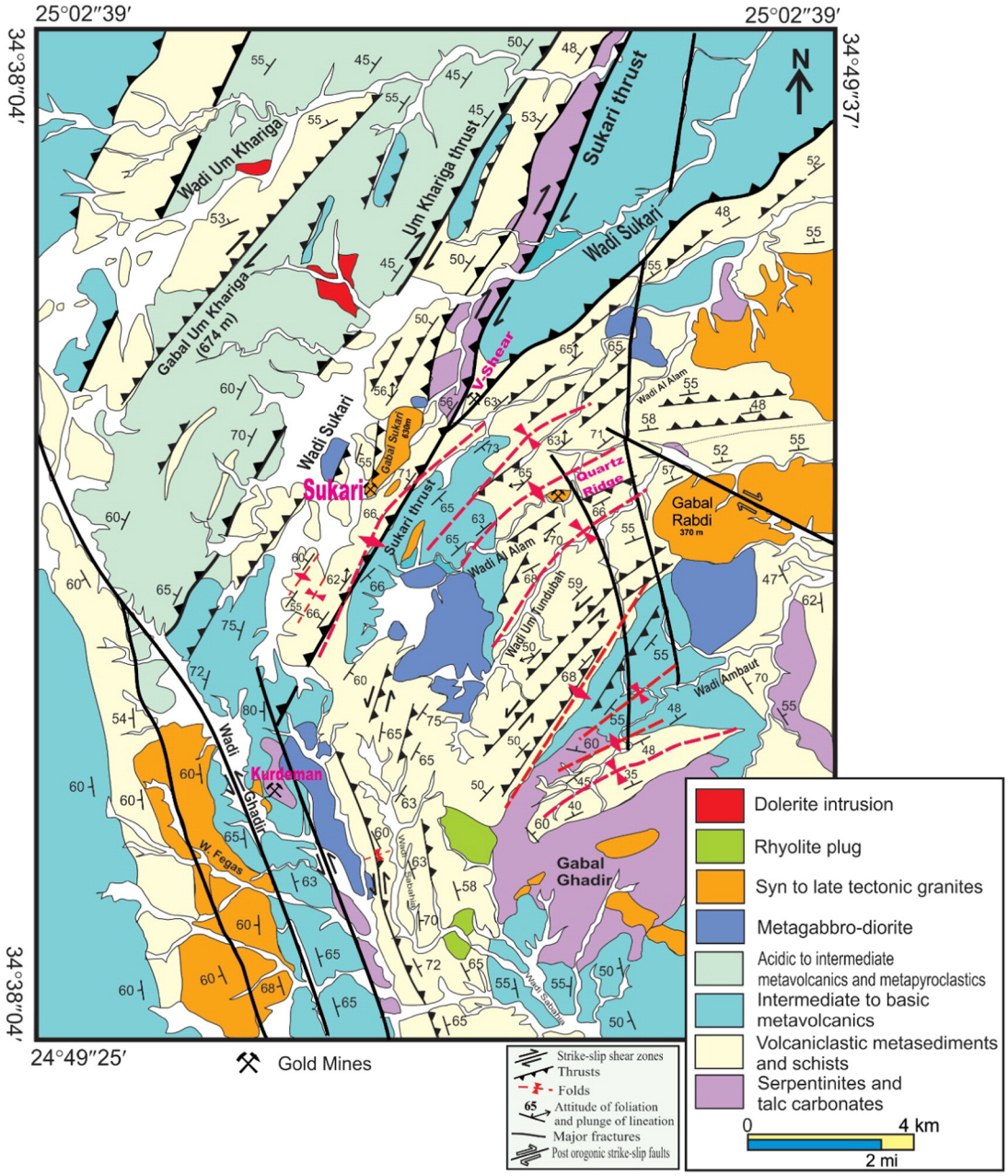

Fig. 3. Geological map of Sukari and Kurdeman mine areas.

island arc assemblages comprising metavolcanics, metapyroclastics and schists.

2.1. Ophiolitic rocks

The ophiolitic sequence, which forms a structurally complex elongate belt in the central and south-western parts of the Sukari area, is made up of imbricate thrust sheets and slices of allochthonous, dismembered remnants of oceanic crust. The original distribution of rock units and pseudostratigraphy was disrupted during emplacement of the island arc assemblages. It typically consists of serpentinite–talc–carbonate and metagabbro–diorite complexes forming detached sheets embedded in a highly tectonized matrix.

The highly sheared ophiolitic rocks are grouped into: a) Fine-grained, yellowish brown talc schists, made up mainly of very small laths of talc with minor chlorite; b) Porphyroblastic talc carbonate rocks, composed of large calcite and magnesite patches in a schistose groundmass of fibrous talc grains; and c) silica-carbonate (listwaenite) rocks, composed essentially of quartz with bands of talc and carbonate. The serpentinites are made up mainly of antigorite admixed with chrysotile and lizardite. Carbonate minerals constitute about 10% of the whole rock and may exceed 80% in the talc–carbonate rocks (Harraz, 1991).

The serpentinite masses and lenses are usually aligned concordantly with the enclosing country rocks. The serpentinites are rather heterogeneous and composed chiefly of sheared serpentinite with talc–carbonate and chrysotile veinlets. Near thrust zones, the serpentinite rocks are listwaenitized and contain sulfide minerals. Weathering of the listwaenitized serpentinite produces a distinctive bright orange color and a hackly surface, on which quartz and carbonate veins show in positive relief relative to the carbonate matrix. The contacts between the serpentinites and enclosing volcaniclastic metasediments are mostly tectonic, whereas the contacts between the serpentinite masses possess an outer periphery of talc–carbonate rocks characterized by cavernous

structures and a whitish buff color. Some of the serpentine clasts within the mélange are oriented in the direction of shearing and surrounded by silicified-carbonatized materials.

2.2. Metagabbro–diorite complex

The metagabbro–dioritic rocks are scattered as isolated bodies within the volcaniclastic metasediments (Fig. 3). They are composed chiefly of hornblende–metagabbros with relict pyroxene, quartz–metagabbros, diorites and quartz–diorites. The rocks are medium- to coarse-grained and gray to greenish gray in color. They consist mainly of andesine–labradorite and augite with subordinate amounts of reddish-brown hornblende. Augite and hypersthene are commonly replaced by actinolite, chlorite and subordinate amounts of quartz and biotite. The metagabbro–diorite complexes are intruded predominantly into the serpentinite–talc–carbonate and overlain by island arc assemblages from volcaniclastic metasediments.

The contacts between the metagabbro–diorites and serpentinite is gradational and display variation in mineralogical composition and textures (Harraz, 1991). A NNE-SSW trending schistosity is observed in metagabbro–diorites at the headwaters of Wadi Al Alam. The metagabbro–diorite complex contains sporadic quartz veins which are usually barren. Quartz veins containing-gold are recorded in intensively altered shear zones occurring in the contact zone between metagabbro–diorite and serpentinites or volcaniclastic metasediments to the west of the Sukari gold mine.

2.3. Metasediments

The metasedimentary sequence forms a low to moderate topography in small tracts beyond the frontal slices of the ophiolites. The volcaniclastic metasediments comprise a thick interbedded sequence of metagreywacke, metasiltstone, metamudstone and mica-schist. The rocks are extremely fine grained, greenish gray to dark gray and contain small boulders and cobbles of quartz–carbonate. The mica-schist and metamudstone are the most abundant varieties. This succession is characterized by presences of a slaty cleavage and incipient schistosity which generally strikes parallel to the bedding and lamination. The bedding is marked either by the alternation of lighter and darker colored bands or by alternating fine and coarse bands of clay minerals with quartz and carbonate materials. The mica-schist is characterized by the prevalence of pencil-like cleavage.

2.4. Metavolcanics

The metavolcanics range in composition from mafic to felsic. They have been classified into metabasalt, metabasaltic–andesites, hornblende-plagioclase schist, and chlorite schist. The metabasalt occurs as fine-grained recrystallized rocks exhibiting evidence of metamorphism under upper greenschist to epidote-amphibolite facies conditions. Near thrust faults, the metabasalts are usually converted into talc-tremolite and chlorite schists. Generally, these rocks are composed essentially of plagioclase, epidote, and chlorite and less common hornblende. In places, epidote, chlorite and albite completely replace the original mineralogy.

2.5. Granites

The Sukari pluton which is the hostrock for gold mineralization has a strike length of approximately 2300 m, and varies in width from 100 m to approximately 600 m (Cavaney, 2005). It is mineralogically heterogeneous and ranges from tonalitic to trondhjemitic composition with dominant quartz, plagioclase and potash feldspars and less abundant biotite (Arslan, 1989; Sharara and Vennemann, 1999; Dawood et al., 2005; Lundmark et al., 2012). The Sukari pluton is well-known for its gold-bearing quartz veins and has been interpreted alternatively as belonging to the older granites (Akaad and Noweir, 1980) as well as younger granite (Sharara, 1999; Helmy et al., 2004). Geochemical evidence suggests that the Sukari pluton was generated by partial melting of metagraywackes at ~800 °C as deduced from zircon saturation temperatures (Dawood et al., 2005). On the basis of Rb—Sr isotope studies, Ghoneim et al. (1999) suggested a crystallization age of 559 ± 6 Ma for the Sukari granite, followed by sodium metasomatism at 520 ± 11 Ma. Lundmark et al. (2012) based on U—Pb data interpreted a magmatic age of 689 ± 3 Ma for the pluton. Therefore, the Sukari intrusion is not, as previously suggested, one of the younger granites. Lundmark et al. (2012) postulated 6 separate pulses of magmatism in the CED and assigned the Sukari pluton to the oldest 705–680 Ma group of syn-orogenic granites. Zircons from three samples analyzed by SHRIMP yielded a magmatic 206U/238U age of about 663–672 Ma (Talavera, 2013).

The Sukari pluton was intruded mostly into the volcaniclastic metasediments and its regional trend is aligned nearly parallel to the regional foliation in the enveloping country rocks (mica schist). The Sukari pluton is generally fine to medium grained with pale pink to gray color, and mostly free of xenoliths. The fresh granitoid rock is leucocratic and coarse-grained.

The contacts between the Sukari pluton and the volcaniclastic metasediments at the western margin of the pluton are sharp intrusive contacts. This sheared contact zone contain the main auriferous mineralized zone at the Sukari gold mine. Elsewhere, the contact between the granitoid and the surrounding country rocks are of tectonic nature, particularly with metagabbro-diorite complexes. The pluton was later intruded by numerous dykes (i.e. dolerite dykes and several felsite dykes) and quartz veins. The dykes and quartz veins intrude both the granite and the country rocks. Drilling indicates that the Sukari Pluton dips toward the east at between 50° and 75° where the western and eastern contacts of the pluton are thus regarded as footwall and hanging-wall contacts respectively (Smith et al., 2014).

The Sukari granite is strongly sheared and foliated and serpentinite is altered to listwaenite rock particularly in the vicinity of shear zones along its outer eastern and western margins. The contacts between the Sukari pluton and wall rock are, in places, vertical or overturned. Jointing in the pluton is rather conspicuous in three main directions: NNE-SSW, NW-SE and NE-SW. The latter direction is only weakly developed and is parallel to the main trend of mineralized quartz veins that are particularly distinctively in the eastern part of the pluton.

The main mineralized lode in the Sukari pluton occurs along the contact between the granite and the volcaniclastic metasediments. The main auriferous quartz vein runs NE-SW along shear fractures for about 450 m, striking 25–35° NE and dipping 30–55° toward the SE and accompanied by a series of en-echelon arrays, veinlets and offshoots suparallel to the main zone. The main quartz vein is 2.5 m thick, milky white and usually associated with sulfides and strong hydrothermal alteration of the volcaniclastic metasediments, on both sides of the mineralized vein.

There are other granitoid bodies within the study area, at Kurdeman and in the east Sukari area, which are characterized by lower relief in comparison with the Sukari granite bodies. These granitoids are gray to whitish in color with medium- to coarse-grained equigranular, hypidomorphic and sometimes foliated textures. Quartz diorites and granodiorites are present at Kurdeman and east Sukari. Granite in east Sukari is of gray color and contains abundant ankerite.

2.6. Dykes

The dykes to the east of Sukari pluton are associated with a distinctly oriented fracture set, forming an ENE-trending swarm about 10 km width, extending to the Red Sea coast. They transect all rock units, trending parallel to the regional cleavage and varying in composition from basic to acidic and with variable extent and thickness, ranging in width from a few centimeters to >3 m. These dykes also show evidences

of post-intrusive tectonic displacement. Dykes are scarce to the west of the Sukari pluton.

3. Structural setting

The structural evolution and deformation style of the Sukari mine area are very complicated in that NW-SE trending tectonic structures in the southwest are overprinted by NE-SW trending structural fabrics to the east and west of the Sukari gold mine. Therefore, based on the mapped structural features, the Sukari structural belt will classified into the Kurdeman shear zone (KSZ), the East Sukari thrust belt and the West Sukari thrust belt. The Sukari Thrust separates between East and West Sukari areas. Geometric and kinematic studies of these faults are fundamental for understanding the structural features and deformation mechanisms of the thrust belts and strike slip shear zones (Fig. 3).

3.1. Kurdeman shear zone (KSZ)

Mineralization at the Kurdeman gold deposit is shear-zone related and lies within the northern continuation of the major Nugrus Shear Zone (NSZ) which marks the northeastern margin of the Hafafit core complex (Fig. 2). The Kurdeman gold mine is both an ancient and currently exploited mine located 9 km SW of the Sukari gold mine. Drilling intersected high grade gold mineralization (8.54 g/t–32.2 g/t Au) associated with smoky gray quartz veins and sulfides (http://www.centamin.com).

The Kurdeman shear zone (KSZ) comprises an association of highly tectonized mafic metavolcanics, serpentinites, talc–carbonate and metagabbro–diorite embedded in a matrix of volcaniclastic metasediments and schists (Fig. 4). The metagabbros are of tholeiitic composition, consisting of lower cumulate pyroxenites and gabbros that pass upwards into massive gabbros (El-Makky et al., 2012). The talc–carbonate rocks and steeply dipping lenses and sheets of serpentinites were emplaced along thrust planes and elongated in NNW-SSE direction parallel to the penetrative foliation of the volcaniclastic metasediments matrix. Schists, talc–magnesite rocks and listwaenite mark the thrust contacts between tectonized serpentinites and other mélange components whereas, chlorite, sericite and carbonate mark the contacts between boudinaged mineralized quartz veins and the enveloping rocks.

NNW-trending spaced foliation and S-shaped asymmetric crenulations are common (Fig. 5a) in volcaniclastic metasediments and talc–carbonate rocks, especially in the high strain zones and near fold closures.

The metavolcanic rocks are folded into a major anticline (Fig. 5b and c) with their axial plane having a moderate dip to the SW and fold axes plunging moderately to the NNW. Also, macroscopic and small scale folds and crenulations were developed in volcaniclastic metasediments especially in the vicinity of the metavolcanics. The NNW-trending schistosity along the western bank of Wadi Sabahia is folded into a low amplitude syncline with axes plunging moderately to the ENE (Fig. 3).

The Eastern part of the KSZ exhibits variably plunging mineral stretching lineations where the NNW-trending schistosity in volcaniclastic metasediments curve into a N- and NNE-trend. In the eastern part of the KSZ, the mineral stretching lineation and the long axis of stretched pebbles in volcaniclastic metasediments are plunging 25–30° toward the NNW (Fig. 6a) and curve toward the SSE and SSW.

The area surrounding the Kurdeman gold mine is dissected by numerous fault sets, varying from reverse (moderate to low angle thrusts) to almost vertical strike-slip shear zones. The thrusts strike mainly NNW-SSE whereas most of the strike-slip shear zones trend NNW-SSE and NW-SE (Figs. 5d and 6b). The thrusts mark the tectonic contacts between the ophiolitic slabs (serpentinites and talc carbonates) and the underlying metavolcanics and metagabbro–diorite (Fig. 5e). The highly sheared talc schists, talc carbonates and listwaenite are commonly associated with thrusts and strike-slip shear zones. In the western and central part of the KSZ, slickenlines are present along shear planes plunging 10–15°/N30°W. Fiber lineations along reverse and thrusts are steeply plunging 52° toward ESE.

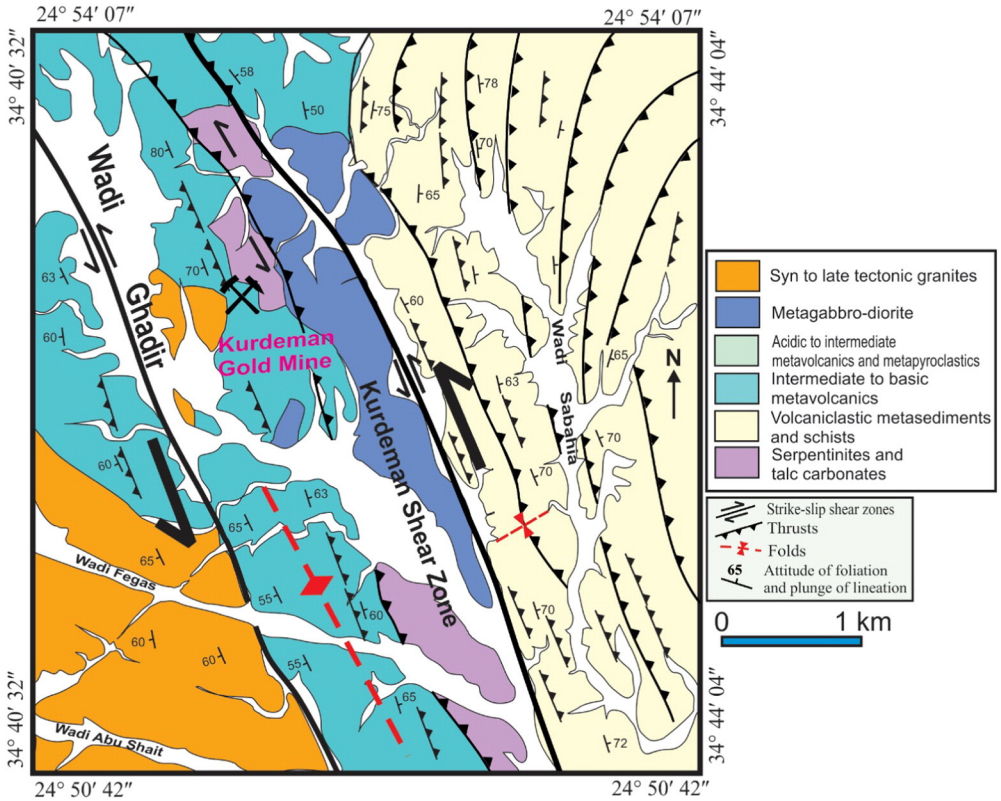

Fig. 4. Geological map of Kurdeman gold mine area.

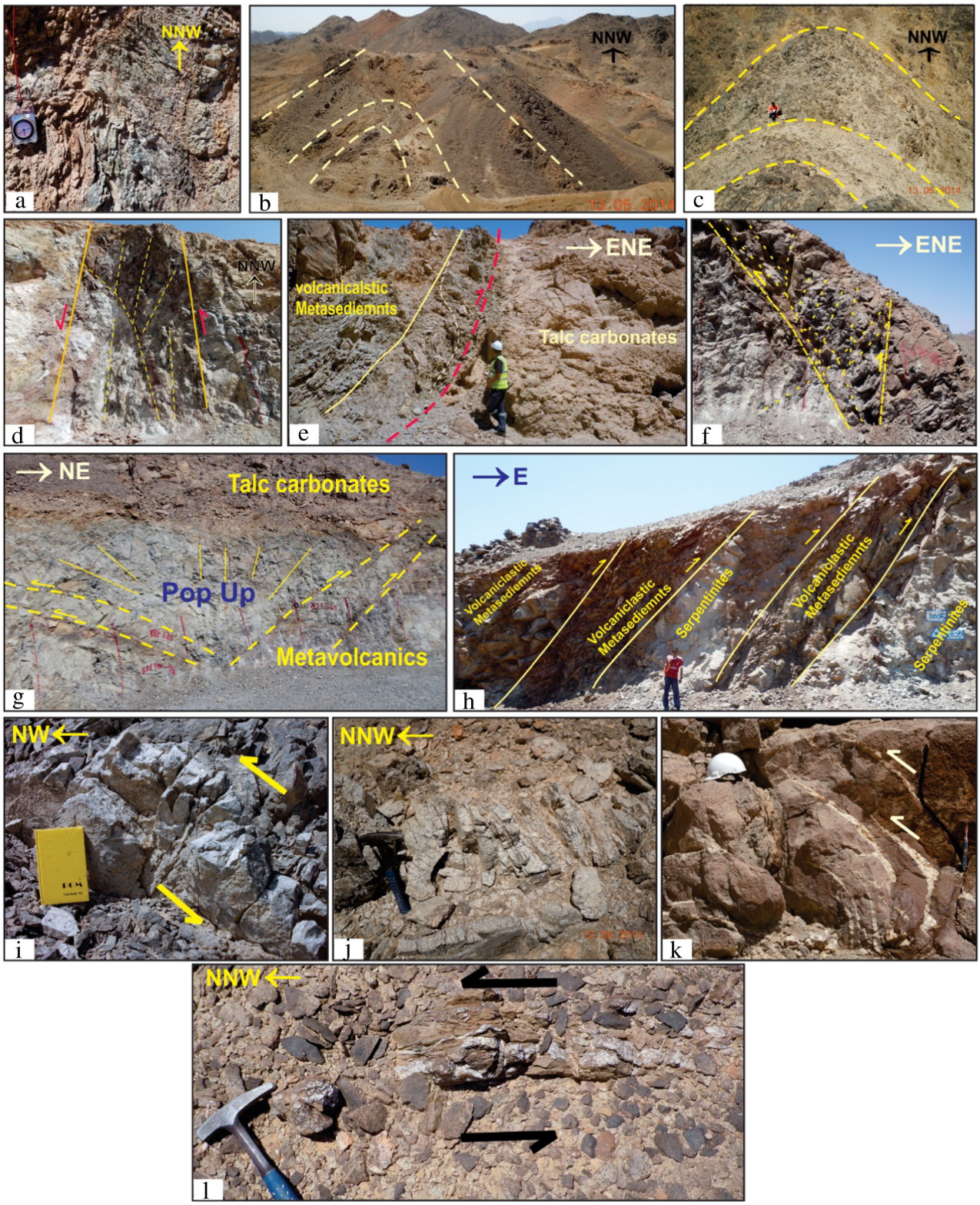

Fig. 5. Structural features from Kurdeman gold mine area. (a) Crenulation cleavage in volcaniclastic metasediments, (b) and (c) NNW-trending anticline in sheared metavolcanics, (d) Vertical NNW-striking strike-slip shear zones, (e) WSW-dipping thrust mark the tectonic contacts between volcaniclastic metasediments and talc-carbonates, (f) Flower-like structure (g) Pop up structure between a pair of oppositely moving conjugate thrusts, (h) Thrust sheets forming an imbricate structure, (i) Barren milky white quartz vein in metagabbro–diorite, (j) Fractured and brecciated quartz vein in Kurdeman shear zone, (k) and (l) Curved and deformed quartz veins in Kurdeman shear zone.

The thrusts in the KSZ show a typical sequence of propagation where each successive thrust develops in footwall of the previous thrust in piggy-back thrust manner. This led to the development of pop-up (Fig. 5f and g) and flower-like structures (Fig. 5f) where a tectonic wedge or block of rocks moved upward antithetically between a pair of oppositely moving conjugate thrusts. The uplifted hanging wall block between the fore (main) thrust and back thrust is the pop-up (Fig. 5g). Such structures are usually associated with flower-like

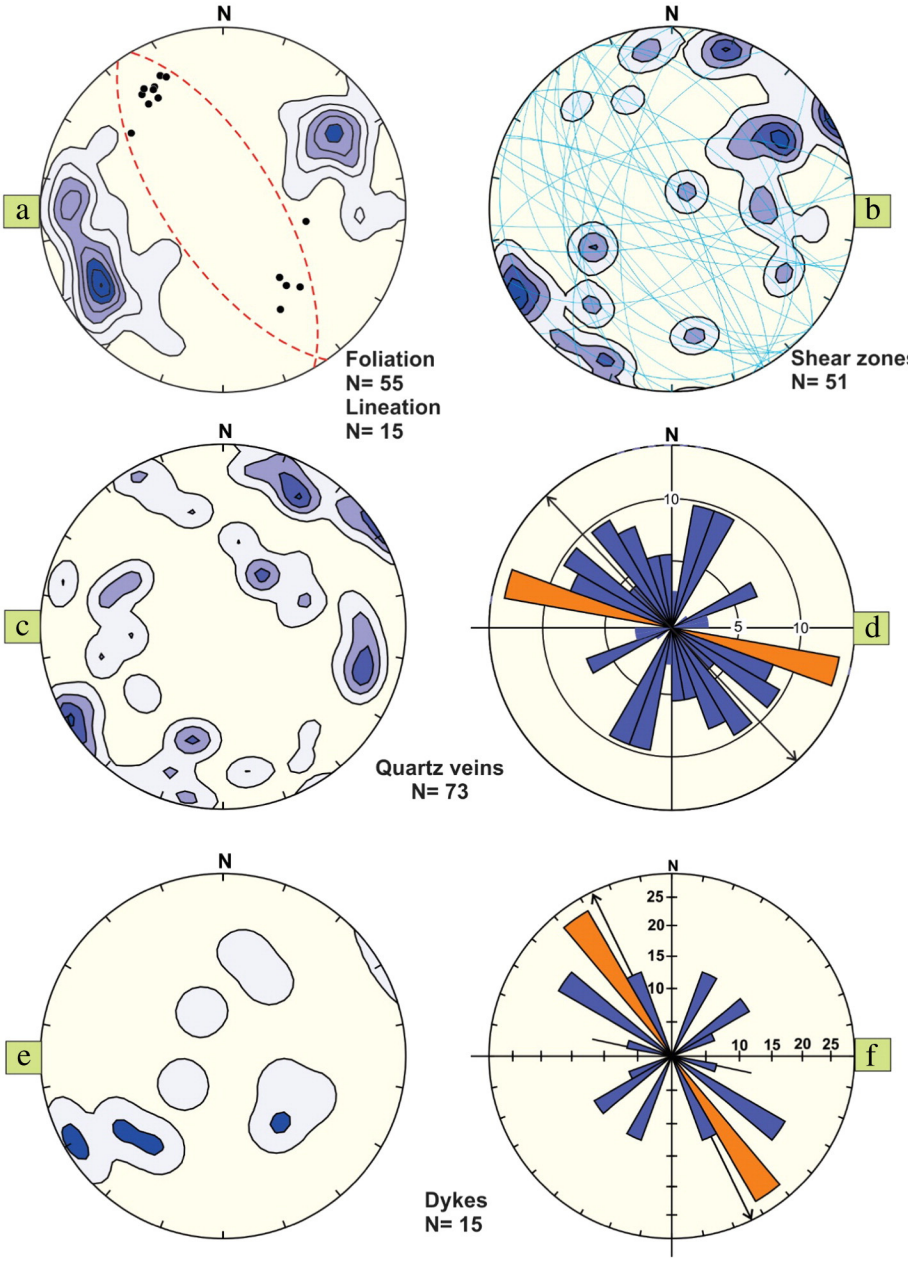

Fig. 6. Structural data from Kurdeman gold mine area; (a) Poles to S_2 foliation, contoured at 0, 2, 4, 6 and 20% per 1% area, and orientations of L_2 lineation; (b) Poles to shear zones, contoured at 0, 2, 4, 6 and 20% per 1% area, (c) Poles to quartz veins, (d) Main trends of quartz veins, (e) Poles to dykes, and (f) Main orientation of dykes.

cleavage and tile-like piling of subsidiary thrust sheets forming an imbricate structure (Fig. 5h).

From the mineralization perspective, two types of quartz veins have been recognized in the Kurdeman area (Fig. 6c and d) depending on whether they are mineralized or non-mineralized. Mineralized quartz veins are mainly hosted in shear zones within metavolcanic rocks. Thick gray, smoky recrystallized quartz are rich in secondary iron minerals. Small-scale open folds are observed in highly deformed quartz veins in talc carbonate rocks.

The exploited veins are concentrated in the 1 km^2 area encompassing the old Kurdeman workings. They trend mostly NW-SE and N—S and dip steeply towards the southwest. These veins range between 10 and 50 cm thick and display splitting and branching behavior. The Kurdeman adit trends NW-SE and dips steeply to the SW. Non-mineralized (barren) quartz veins are milky white and represent the dominant vein type (Fig. 5i and j) in the Kurdeman area. They are particularly abundant in the metagabbro-diorite rocks. They trend mostly NNW-SSE with fewer veins trending NE-SW and dip both NE and SW. Some of the non-mineralized quartz veins are displaced by small-scale NE-trending dextral shear zones. Some other veins are folded and low amplitude folds developed (Fig. 5k and l).

It is also noteworthy that calcite veins oriented parallel to the quartz vein sets but at a distance of 0–10 m away from them; some calcite veins extend >300 m toward N-S or NNW-SSE.

Dykes in the Kurdeman area vary in composition from basic to acidic and vary in their extent and thickness. All dykes trend NW-SE and dip to the SW and less commonly to the NE (Fig. 6e and f). Basaltic dykes are intruding the metavolcanic rocks whereas, acidic dykes intruded metagabbro-diorite and ultramafics rocks.

Some NE-striking high angle normal faults were detected in the metavolcanic rocks and metagabbro-diorite. They represent the latest brittle deformation event in the Kurdeman gold mine area.

The KSZ is interpreted to have undergone reverse oblique slip, which consistent with transpressional shear zones where mineral stretching

lineations can vary continuously from horizontal to subvertical. A series of splay faults branching off and ramping sequentially out of the main KSZ form an imbricate thrust fan. This thrust fan propagates from the KSZ and extends to the east of the Sukari gold mine, forming the east Sukari thrust fan.

3.2. The East Sukari thrust belt

East Sukari area is bounded by Sukari Thrust and the KSZ and occupied mainly by highly tectonized serpentinites, volcaniclastic metasediments, intermediate to mafic metavolcanics, metagabbro–diorite and intruded by syn-orogenic granites and numerous dykes.

The regional foliations strike NNE-SSW close to the KSZ but curve into a NE-SW direction around Wadi Al Alam, Wadi Um Tundubah and Wadi Anbaut, and then into an ENE-WSW trend to the south of Gabal Rabdi (Fig. 3). The metavolcanics show increasing effects of deformation with development of a strong foliation defined by chlorite, actinolite fibres and granular epidote (metabasalts). Intensity of cleavages varies throughout the East Sukari area. Steep crenulation cleavages (65°–80°) with an approximate NE-SW strike occur along the gently NW-dipping limbs of the major folds and within high strain shear zones. Moderately dipping crenulation cleavages occur on the overturned limbs of the regional asymmetric folds or in the gently dipping, intensely foliated parts of the fault zone.

Talc–carbonate, talc–chlorite and chlorite schists are strongly foliated, with the foliation defined by the alignment of chlorite, sericite, quartz and talc in schist and aligned actinolite in basic metavolcanic rocks. Discrete and zonal types of crenulation cleavage are developed parallel to the axial planes of major folds. Mylonitic foliation occurs in the central parts of the high-strain zones or along narrower and discrete high-strain zones. The steeply dipping mylonitic foliation has a sigmoidal trend within the strike slip shear zones. The mylonitic foliation is folded and crenulated around small-scale M and Z folds. Poles to foliation showing moderately developed clusters and tend to strike N20°–75°E with dips of 55°–75° toward NW and SE (Fig. 7a and b).

The East Sukari area is defined as a series of map-scale relatively open, high-amplitude, northeast-trending anticlines and synclines which have a general asymmetry with steep fore-limbs and back-limbs (Fig. 8a). Their fold axes trend mainly parallel to the major northeast trending valleys (e.g. Al Alam, Um Tanduba and Anbaut). Major anticlines and synclines are spaced at approximately 2–4 km intervals and have wavelengths of up to 3 km. Axes of these folds plunge 45°/S50°W (Fig. 7a). Increasing tightening of folds is associated with intensification of cleavage to a pervasive foliation and transition from upright folds to inclined and overturned folds. Axial planes of these folds mostly have moderate to steep dips to the NW although occasionally they are to the SE with axes plunging moderately to the NE and less commonly SW. The fold axes appear to swing from NE- to ENE-trending and change from inclined plunging folds to recumbent folds with reclined geometry where overprinting produces complex refolding.

Minor folds are abundant in schists and less common in metavolcanics and absent in metagabbros. These minor folds are tight to isoclinals with

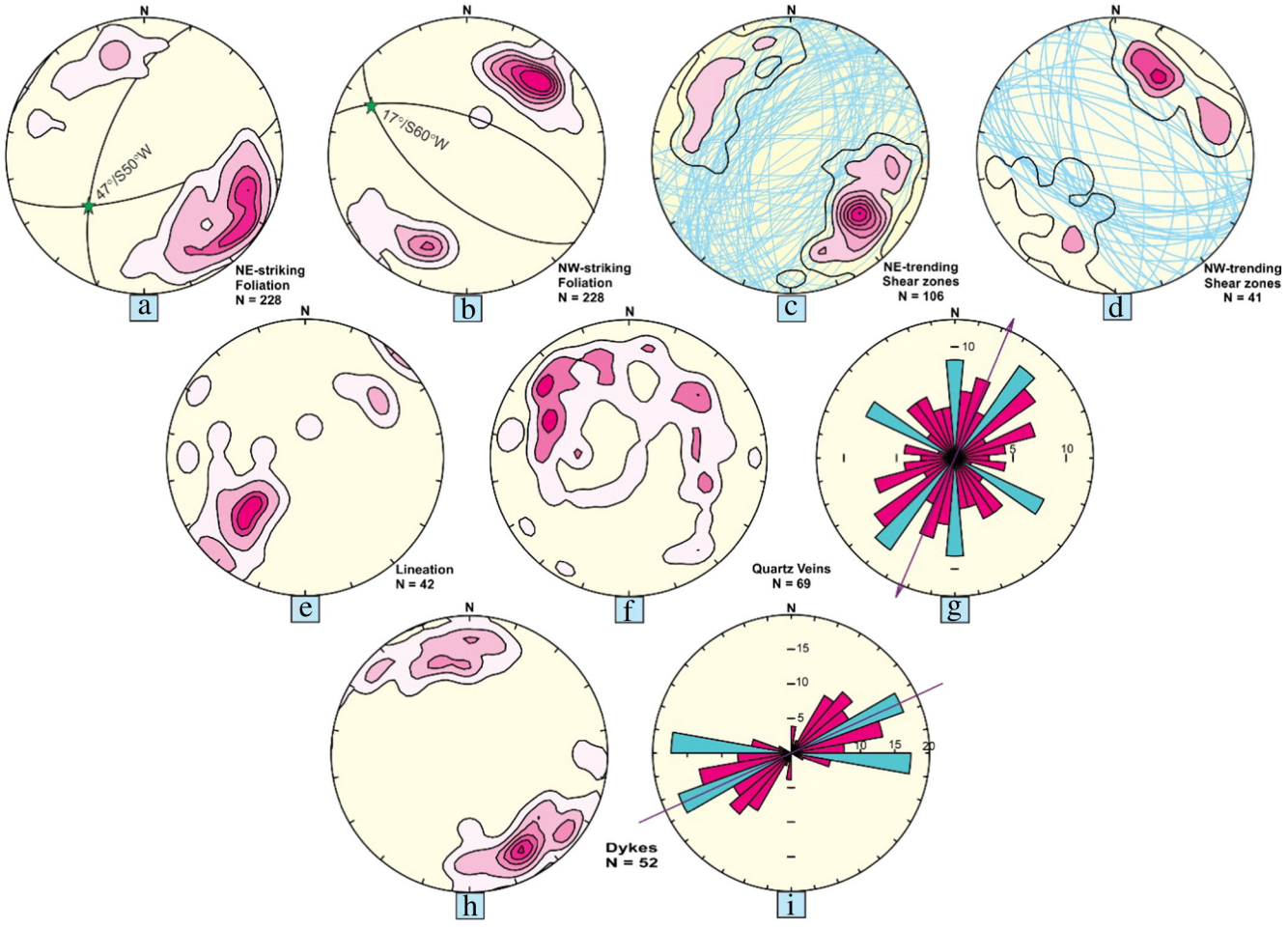

Fig. 7. Structural data from East Sukari shear belt: (a) and (b) Equal area lower hemisphere for poles to NE- and NW-striking foliation showing moderately developed clusters with non-uniform distribution, (c) and (d) Poles and great circles to shear zones showing moderately developed clusters with non-uniform distribution, (e) Measured linear structures along the planes of thrusts and strike slip shear zones, (f) Equal area lower hemisphere for poles to quartz veins, (g) Rose diagram showing main trend of quartz veins, (h) Equal area lower hemisphere for poles to dykes, and (i) Rose diagram showing main trend of dykes.

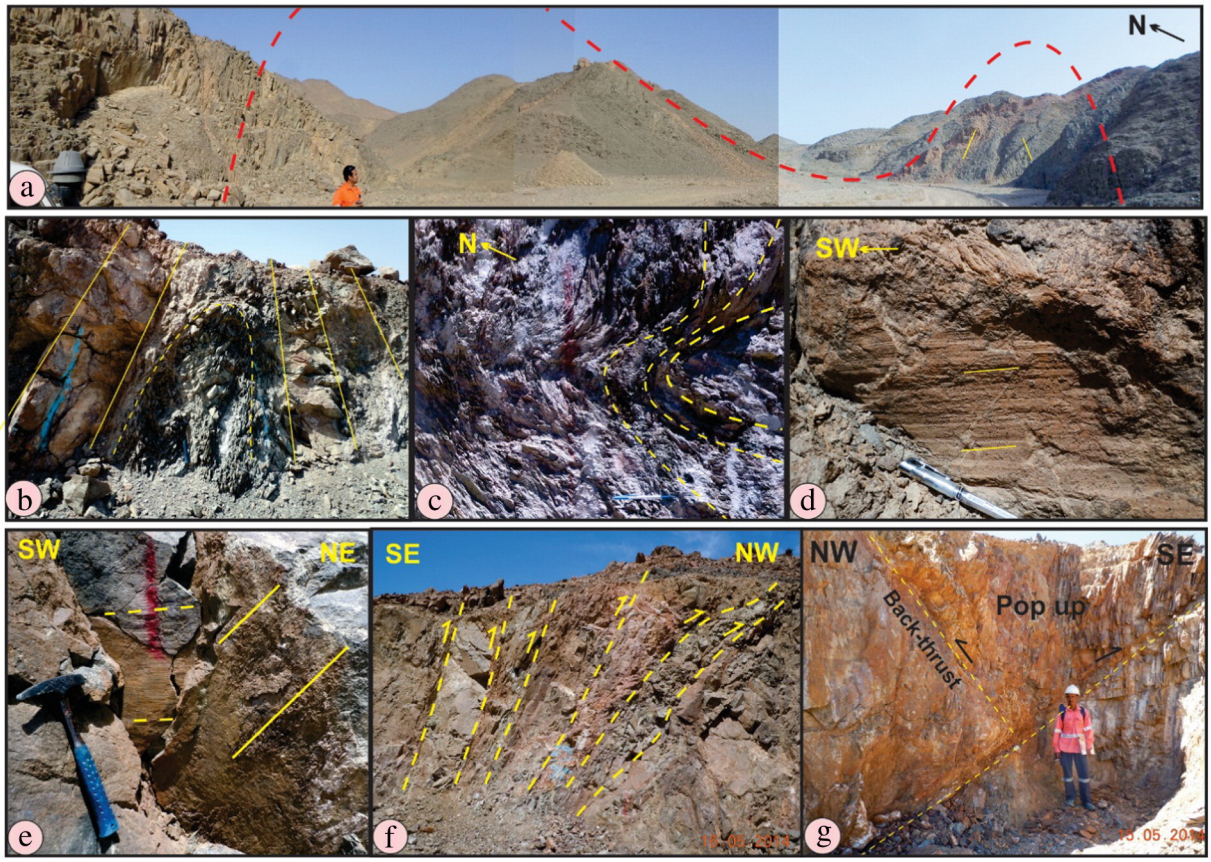

Fig. 8. Structural features from East Sukari shear belt. (a) Map-scale broad relatively open, high-amplitude, northeast-trending anticlines and synclines along Wadi Al Alam, (b) NE-trending tight to isoclinals fold with rounded hinge, (c) Recumbent fold in volcaniclastic metasediments, (d) Lineation plunging gently to SW in mylonite schists along Wadi Al Alam (e) Sub-horizontal slickensides overprinted by steeply dipping striae in sheared metavolcanics along Wadi Al Alam, (f) Northwest-side-up imbricate thrusts in volcaniclastic metasediments along Wadi Um Tundubah, and (g) Uplift bounded by two oppositely directed thrust faults forming pop-up structure.

angular hinges in schist (Fig. 8b and c) whereas angular to rounded hinges occur in metavolcanic rocks. Tight folds occur in schists and volcaniclastic metasediments whereas low amplitude folds with parallel geometry occur in sheared metavolcanics.

The stretching lineation is contained within the intense mylonitic foliation and is defined by elongate and extended biotite, quartz ribbons and feldspar porphyroclasts. Moderately to steeply plunging down-dip mineral lineations defined by amphibole needles and elongate clots of quartz and feldspar is conspicuous within the plane of mylonitic foliation in schist and highly sheared metavolcanic rocks. The rock fragments and porphyroclasts in different types of schists are elongated parallel to the down-dip lineation (Fig. 7e). Also, the pinch and swell produced by boudinage of quartz veins, axes of minor folds and grooves and ridges on the surface of the quartz veins are parallel to this lineation. Therefore, the observed linear structures along thrust planes represent the direction of maximum elongation on the plane of foliation.

Some high-strain strike-slip shear zones occur along Wadi Al Alam and Wadi Um Tundubah. They are mainly fine-grained highly sheared metavolcanic rocks and mylonite schists and show the ubiquitously steeply dipping foliation and shallowly south-westerly plunging lineation (Fig. 8d). Sub-horizontal slickensides overprinted by steeply dipping striae are common (Fig. 8e).

The NE- to ENE- and scarce NW-trending thrusts (Fig. 7c and d) define the tectonic contacts between the volcaniclastic metasediments and schists and the underlying metavolcanics and metagabbro–diorite. Quartz veins, talc carbonates and listwaenite are commonly associated with the thrusts. The East Sukari area is marked by a series of closely related branching arrays of imbricate thrust faults and overlapping fault-propagation folds forming an imbricate thrust fan. The East Sukari thrusts are forward-breaking or "piggy-back thrust" sequence thrusts where the newer thrusts nucleate in the footwalls of older thrusts and verge in the same direction as the older thrusts (McClay, 1992). The imbricate thrusts (Fig. 8f) are marked by SE and NW-side-up thrust movements and show two structural geometries: the pop-up structures (Fig. 8g), i.e. an uplift bounded by two oppositely directed thrust faults (moving away from each other) and triangle zones (Fig. 8g and 9a), i.e. a depression bounded by two oppositely dipping thrust faults. Most thrusts have a steeply NW-dipping mylonitic foliation with vergence to the northwest. Some other thrusts are SE-dipping indicating derivation from the overturned eastern limbs of the regional asymmetric anticlines. Contacts between units are strongly foliated shear zones up to 100 m wide showing augen structures and S-C fabrics with southeast- and sometimes northwest side-up thrust movements.

Gold occurrences along the East Sukari thrust fan such as the V-shear and Quartz ridge (Fig. 3) prospect areas (local names applied by Centamin Egypt Ltd) are hosted by steeply dipping quartz veins associated with anastomosing mylonitic shear zones. Nothing has been documented concerning ancient or colonial mining activities, although old workings, some Roman ruins have been found. Hydrothermal alteration, strain, and mineralization at these gold occurrences are largely restricted to within host shear zones. V-shear is located 3 km NE of the main Sukari Thrust whereas Q-ridge is along Wadi Al Alam (Fig. 3). Quartz veins in the V-shear area vary from N-S to NE-SW. Individual quartz veins range in width between 10 cm and 3 m and may extend discontinuously for >30–40 m (Fig. 9b and c) and dip to the NW and SE (Fig. 7f and g). They are not related to specific rock types. Veins are milky white with limonite infill was found in some veins and carbonate ankerite in others. Quartz veins in the Quartz Ridge area are nearly vertical, boudinaged (Fig. 9d), folded (Fig. 9e) and sometimes have augen shape or en-echelon arrangement (Fig. 9f). Grooves and ridges

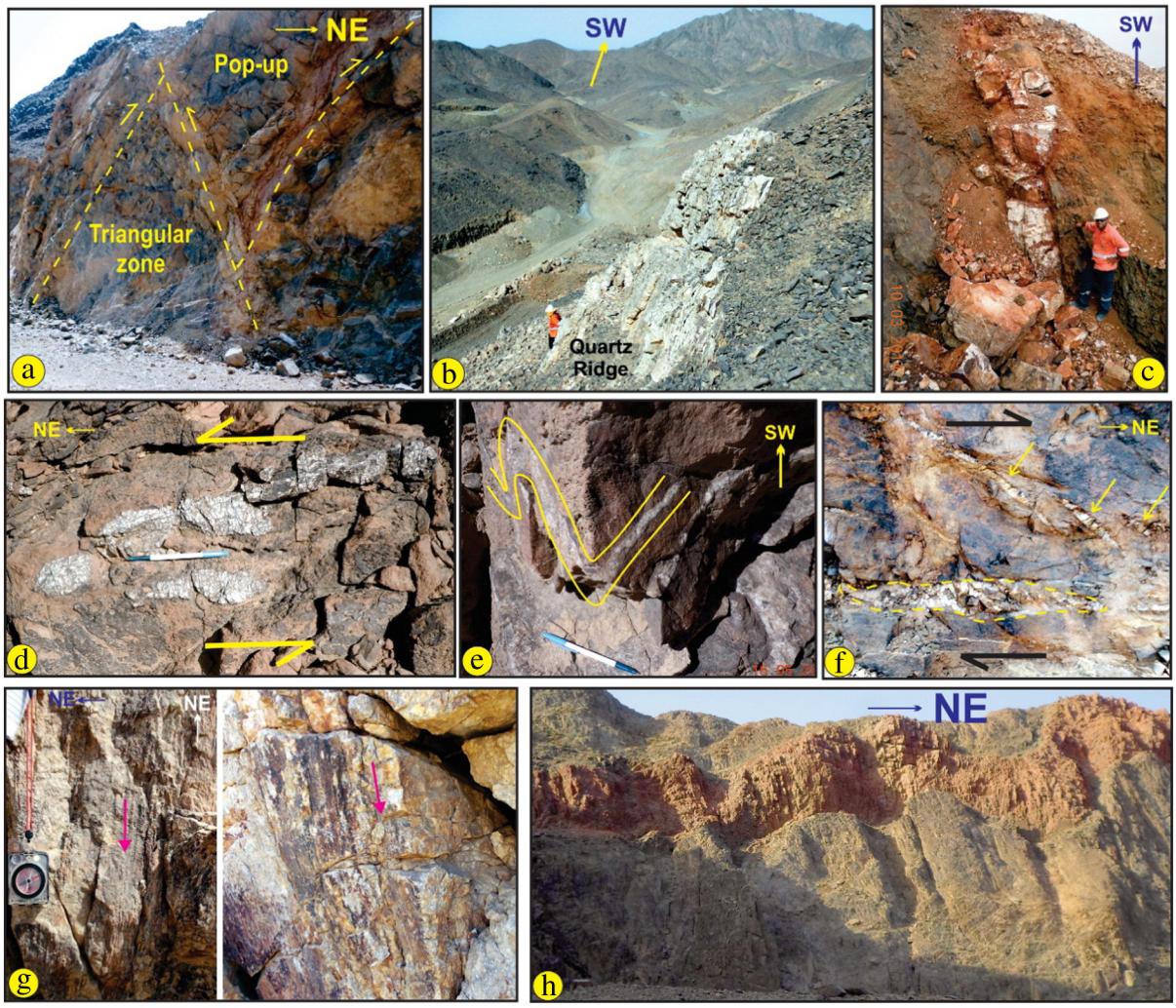

Fig. 9. East Sukari shear belt. (a) Pop up and depression bounded by two oppositely dipping thrust faults forming triangular zone in sheared metavolcanics, (b) and (c) NE-trending thick mineralized quartz veins along Wadi Um Tundubah, (d) Boudinaged quartz vein, (f) Folded quartz vein, (f) Augen shape and en echelon arrangement of quartz veins, (g) Grooves and ridges along the main Quartz ridge parallel to the down-dip lineations, and (h) Displaced and highly fractured felsic dyke traversing volcaniclastic metasediments.

(Fig. 9g) along the main quartz vein are parallel to the down-dip lineations. Limonite and carbonates are common as infillings. High grade assays was returned from the ENE-trending milky quartz vein (400 m long) and sheared gabbro–diorite at Quartz Ridge area (http://www.centamin.com).

Numerous dyke sets traverse the metasediments and metavolcanics in the Sukari area. The dykes have various extent and thickness, but most have a strike length from less than 1 m up to 500 m, and thickness from 0.3 m up to 3 m. They occur frequently as parallel to sub-parallel arrays but sometimes they are irregular (i.e. dykes filling fractures). They are more resistant to weathering than the surrounding country rocks. On basis of their field relationships, they are categorized into felsic and mafic dykes.

The felsic dykes form ENE-trending sets (Fig. 7h and i), and commonly occur near exposures of the Sukari granite. In hand specimen, they are pink colored porphyritic, with feldspar phenocrysts embedded in a fine-grained quartz, sericite and chlorite-rich groundmass. In places, these dykes are displaced or exhibit some evidence of deformation (Fig. 9h). In the Sukari gold mine area, numerous sheets of dacite dissect the host rocks. They are mostly conformably with the foliation planes, and hence considered sills. They vary in width from some decimetres to more than two metres. Flow texture is represented by abundant brown mica flakes, commonly aligned parallel to the sill margins.

The mafic dykes are common as NNE-SSW and/or NE-SW striking swarms in East Sukari thrust belt, traversing the metavolcanic and metasedimentary rocks. The length of some dykes reaches 1000–1500 m. Dykes often branch and rejoin each other. In thin sections, they are basaltic to andesitic in composition, and consist of essential plagioclase, calcite, epidote and chlorite, and minor quartz and iron oxides. Plagioclase occurs as fine acicular laths showing multiple twinning but many crystals are severely altered into kaolinite (Harraz, 1991).

The majority of dykes contain considerable amounts of lenticular quartz veinlets, comprising 5–15% of the volume of the rock. The veinlets are usually of subhorizontal orientation, as a result of which subvertical dykes require the form of “Ladder lodes”. The thickness of quartz veinlets is from a few millimeters to 10–20 m. Along dyke contacts enclosing schists are often silicified, carbonatized, and sulphidized. Small granitic dykes are often schistose, while dykes and stocks are schistose near the contacts (Azzaz, 1987).

3.3. The West Sukari thrust belt

The Sukari granite is elongated in a NNE direction, bounded from west and east by two steep shear zones and dissected by numerous quartz veins (Fig. 3 and 10a). Within the volcaniclastic metasediments, a major NNE-SSW foliation trend corresponds to a high strain zone parallel to the Sukari Thrust, separating the Sukari granites from the

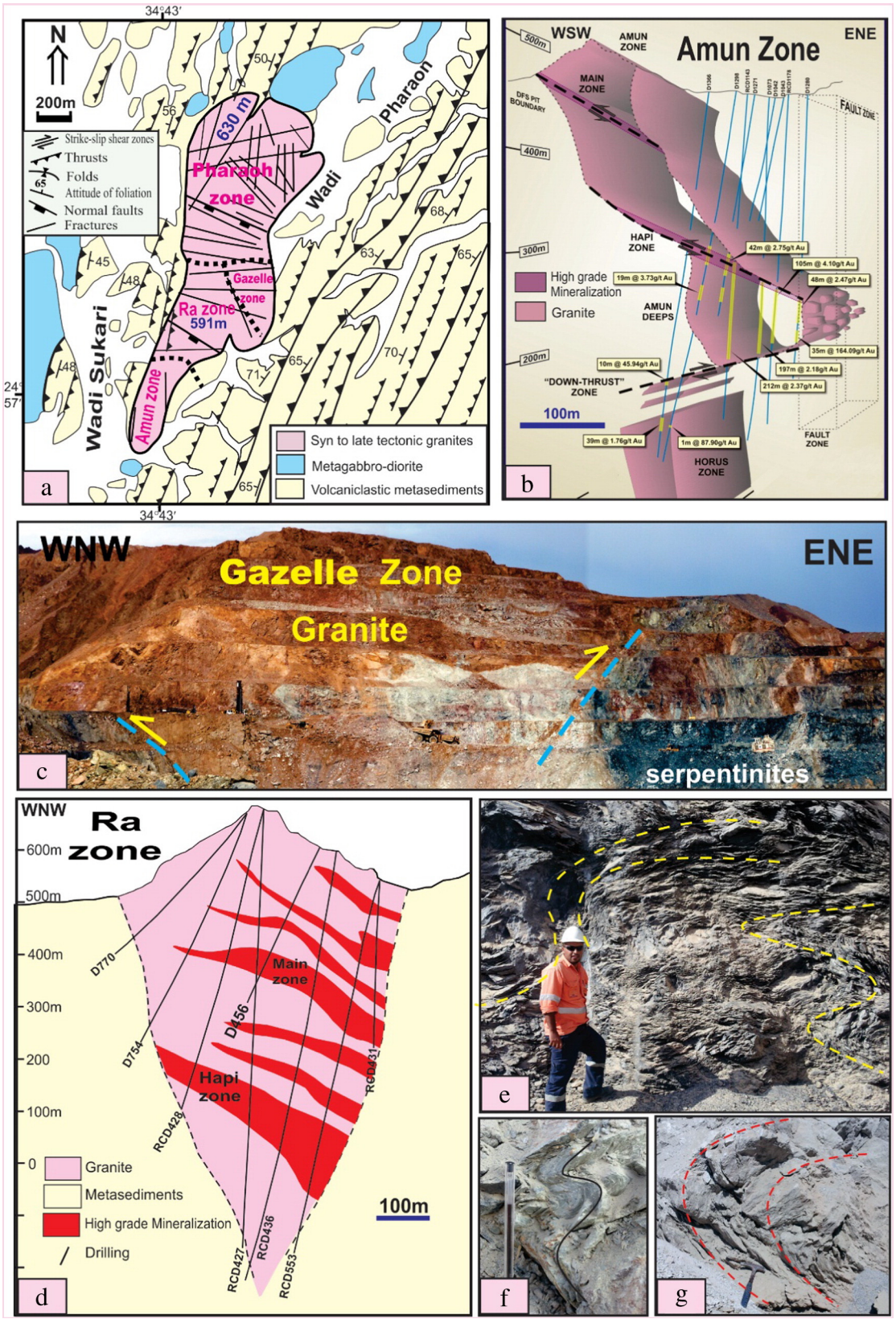

Fig. 10. (a) Geological map of Sukari granite showing main structures and geologic domains, (b) Cross-section along Amun zone showing high mineralizing zones and displacement of granite at depth (after Smith et al., 2014), (c) Photo from Gazelle zone showing oppositely dipping thrusts marking the western and eastern contacts of Sukari granite with serpentinites, (d) Cross-section along Ra zone showing high mineralizing zones and shrinkage of thickness of granite with depth (modified after Smith et al. (2014)), (e) Foliation overprinted by NNE-trending crenulation cleavages forming symmetrical and asymmetrical microfolds, (f) Non-cylindrical and asymmetrical folds, and (g) Recumbent to gently or moderately overturned fold have an axial plane orientation of N25° E, 40–60° NW.

volcaniclastic metasediments to the west and southeast (Fig. 10c). Centamin Egypt Ltd divided the Sukari pluton into four geologic domains from north to south; Pharaoh, Gazelle, Ra and Amun (Figs, 10a–d). In the Amun zone (Figs, 10a and b), the high grade gold assay results were intersected in hole RCD1221 recording 21.83 g/t Au from 549 m and 58.58 g/t Au with visible gold from 559 m. Cross sections show that the thickness of granite decreases with depth and the pluton has been displaced by deep thrusts (Fig. 10b and d).

Most of the S-tectonites of the West Sukari thrust belt consist of volcaniclastic metasediments, schists, serpentinites, acidic to intermediate metavolcanics, metapyroclastic rocks and quartz veins. The foliation of this belt is sub-parallel to parallel with the Sukari thrust and recognized as a continuous schistosity which is characterized by planar fabric elements of layer silicates or flattened/stretched grains that have a preferred orientation and are distributed throughout the rocks. Measurements of the foliation show a mean strike of N15°E, steeply dipping both to the WSW and ENE. This foliation is overprinted by NNE-trending crenulation cleavages forming symmetrical and asymmetrical micro folds (Figs. 10e and 11a). Foliation developed along the strike slip shear zones and thrusts is marked by formation of S/C shear band cleavages. The foliation is weakly developed in the granitic rocks relative to that in the volcaniclastic metasediments, although it still has the same approximate trend of foliation in the area.

Small-scale and large-scale non-cylindrical and asymmetrical folds within West Sukari thrust belt are predominant in volcaniclastic metasediments and schists close to the Sukari granites. They vary from asymmetrical, recumbent to gently or moderately overturned (Fig. 10f and g) and have an axial plane orientation of N25°E, 40–60° NW and SE, parallel with the thrusts and shear zones.

Various types of stretching lineations formed in the west Sukari area during ductile deformation, including a stretching lineation in the mylonite, sheared metavolcanics and sheared margins of Sukari granite. They are defined by the long axes of ellipsoidal quartz grains and long narrow quartz ribbons, and fold hinge lines of mesosopic folds. The main trend of the stretching lineation is N-S throughout the area where the mean plunge and trend of the stretching lineation of elongated quartz grains is 10–30°/N5–15°E to 32°/S10–40°E with a sub-horizontal (10°) to intermediate (40°) plunge (Fig. 11d).

The Sukari gold mine working cuts provide cross-sectional views for different structures since they oriented roughly perpendicular to the strike of these structures. The exposed structures are imbricate stacks of NNE-striking, NW- and SE-dipping thrusts, several fault-bend folds,

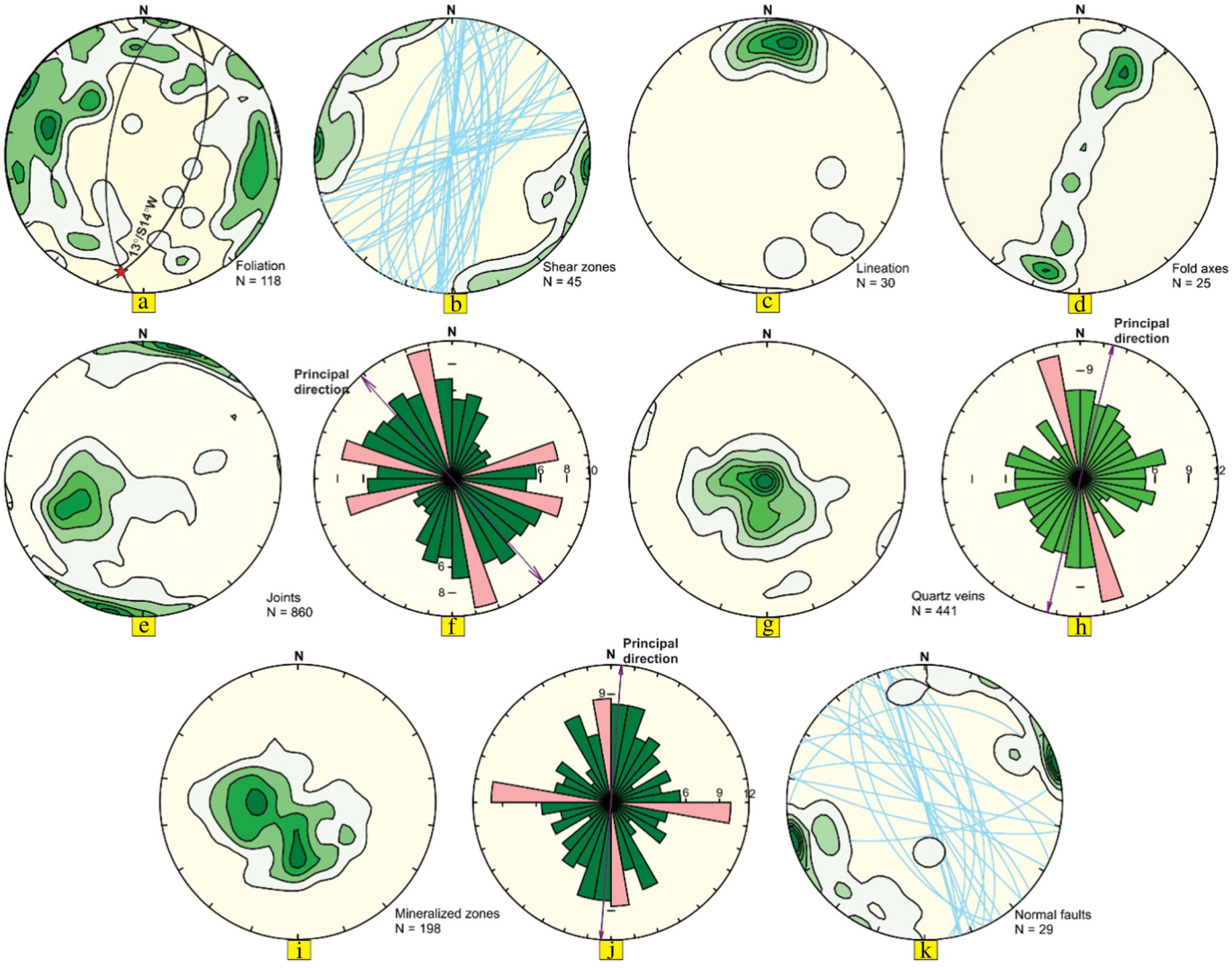

Fig. 11. Structural data from Sukari shear zone: (a) Equal area lower hemisphere for poles to NNE-striking foliation showing moderately developed clusters with non-uniform distribution, (b) Poles and great circles to shear zones, (c) Mineral lineation along the planes of thrusts and strike slip shear zones, (d) Poles to fold axes, (e) Equal area lower hemisphere for poles to joints, (f) Rose diagram showing main trend of joints, (g) Equal area lower hemisphere for poles to quartz veins, (h) Rose diagram showing main trend of quartz veins, (i) Equal area lower hemisphere for poles to mineralized zones, (j) Rose diagram showing main trend of mineralized zones, (k) Poles and great circles to NNW-striking normal faults.

pop ups and strike slip shear zones (Fig. 11c). The Sukari shear zone consist of many of thrust sheets that developed into several imbricate thrusts which merge so as to constitute straight thrust segments. They possibly form a single shear zone and represent segments of Mubarak-Baramiya shear belt (MBSB) described by Abd El-Wahed and Kamh (2010) and Abd El-Wahed (2014). The MBSB is NE-striking dextral strike-slip shear belt that is linked with transpressional imbricate fans and oppositely dipping thrusts.

The Sukari Thrust zone extends in a NNE direction for more than 20 km long with a width of 5 km. Volcaniclastic metasediments, schists, lenses and sheets of serpentinites constitute the hanging wall domain of the Sukari thrust and footwall of Um Khariga thrust. The Sukari thrust zone displays NNE-SSW trend and dips toward both NW and SE. The volcaniclastic metasediments and mafic metavolcanics in the East Sukari thrust fan are the footwall of Sukari thrust (Fig. 12a). The Sukari granite occurs within the hanging wall belt of the Sukari thrust with its long axes trending parallel to the regional foliation and dipping 50–70° to the east (Smith et al., 2014). The eastern and western outer margins of Sukari pluton are strongly sheared compared with its central parts. Parallel sheets of N-striking and E-dipping thrusts containing deformed granites and thinned and stretched quartz veins, felsic dykes and hydrothermal alteration occur at the western margin of the Sukari granite (Fig. 12b, c and d). Thrusted granites masses are accompanied by metapyroclastic rocks, and a series of thrusts faults, readily traceable by fissures between the volcaniclastic metasediments and granites with a wide distribution of multistage dyke intrusions. The eastwards dip of the Sukari granite and thrusting of some granitic masses over volcaniclastic metasediments (Fig. 12e) suggest that the Sukari pluton was emplaced along a back-thrust and displaced by the major Sukari Thrust.

The felsic to intermediate metavolcanics and metapyroclastic rocks from the hanging wall of the NNE-trending and WNW-dipping Um Khariga thrust. Within the Um Khariga thrust zone there are no micro folds and the stretching lineations are parallel to sub-parallel with the strike of the foliations and sometimes significantly oblique or down-dip. The stretching lineation plunges are shallow in proximity to the Um Khariga thrust and they steepen progressively towards the Sukari Thrust zone.

Extensional structures in the Sukari granites (i.e. normal faults) and small scale fractures (i.e. Joints) have a predominantly NW-SE trend (Figs. 11k and 13a), and subordinate trends to the NE-SW, N-S and ENE-WSW (Fig. 11e and f). Two main sets of normal faults striking NW-SE and NE-SW cut the Sukari pluton (Fig. 13a). A series of parallel NW-trending and steeply SE-dipping step faults displaced the Sukari pluton in the same direction (Fig. 13a). Stepwise fault propagation divided the pluton into substantially deformed and rotated blocks. The cross cutting pattern of the joint systems indicates that the NW-SE and the N-S joint system are the older and the NE-SW joint system is the younger. At the intersection of NE- and NW-trending shear zones, where the gold mineralization is concentrated, the Sukari granite is almost completely altered and transected by numerous quartz veins. The older NW-SE shear trend is associated most of the dolerite dykes and some of the milky quartz veins. The NE-SW trend is weakly developed and is occurs preferentially in the eastern part of the Sukari granitic body. The high grade of gold mineralization in the Main Zone and Hapi Zone (local names used by Centamin Egypt Ltd in Sukari Gold

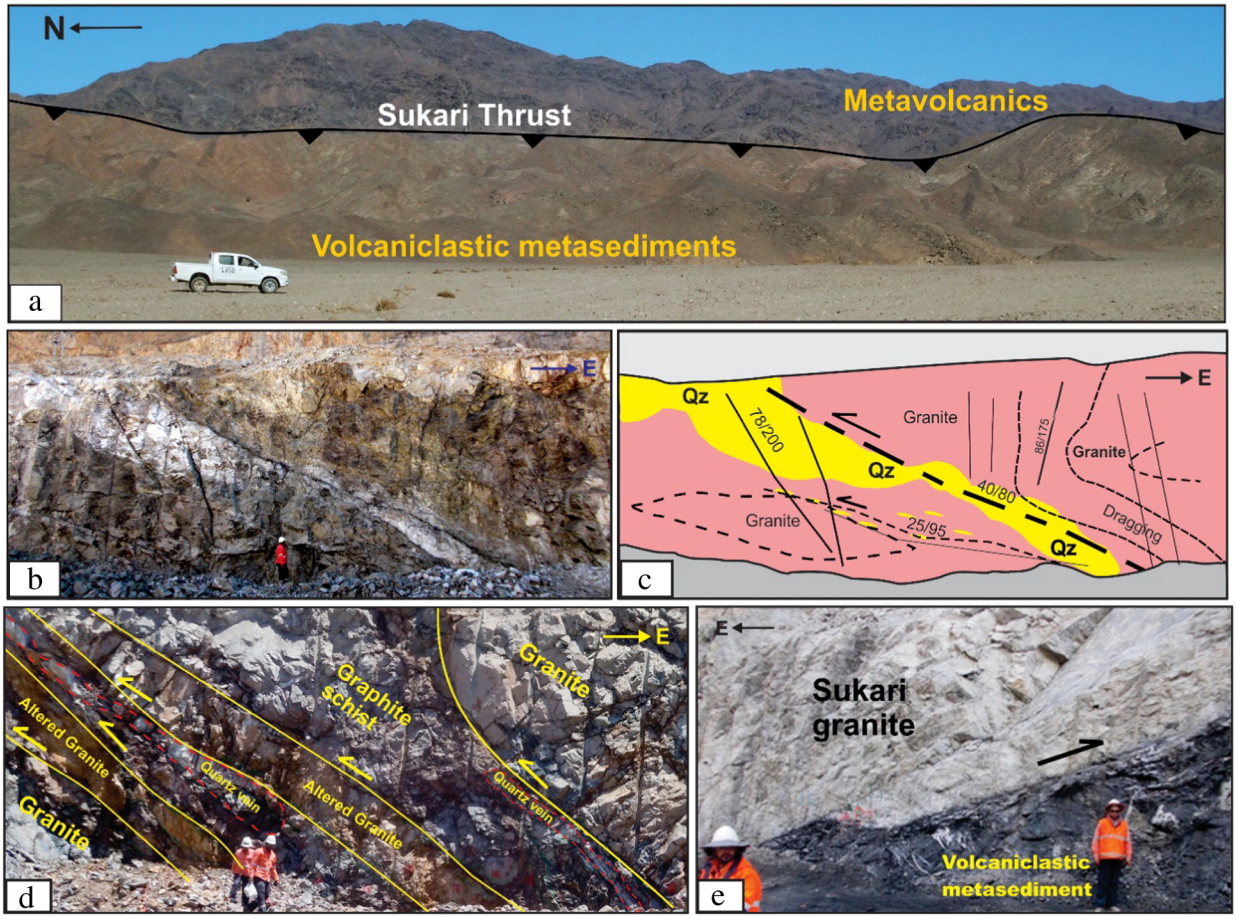

Fig. 12. Structural features from West Sukari shear belt: (a) WSW-dipping Sukari Thrust between basic metavolcanics and volcaniclastic metasediments, (b) and (c) Sheets of E-dipping thrusts containing deformed granites and thinned and stretched quartz veins and hydrothermal alteration exist in the western margin of Sukari granite, (d) Parallel sheets of N-striking and E-dipping thrusts containing deformed granites and thinned and stretched quartz veins, felsic dykes and hydrothermal alteration, and (e) Thrusting of Sukari granite over volcaniclastic metasediments.

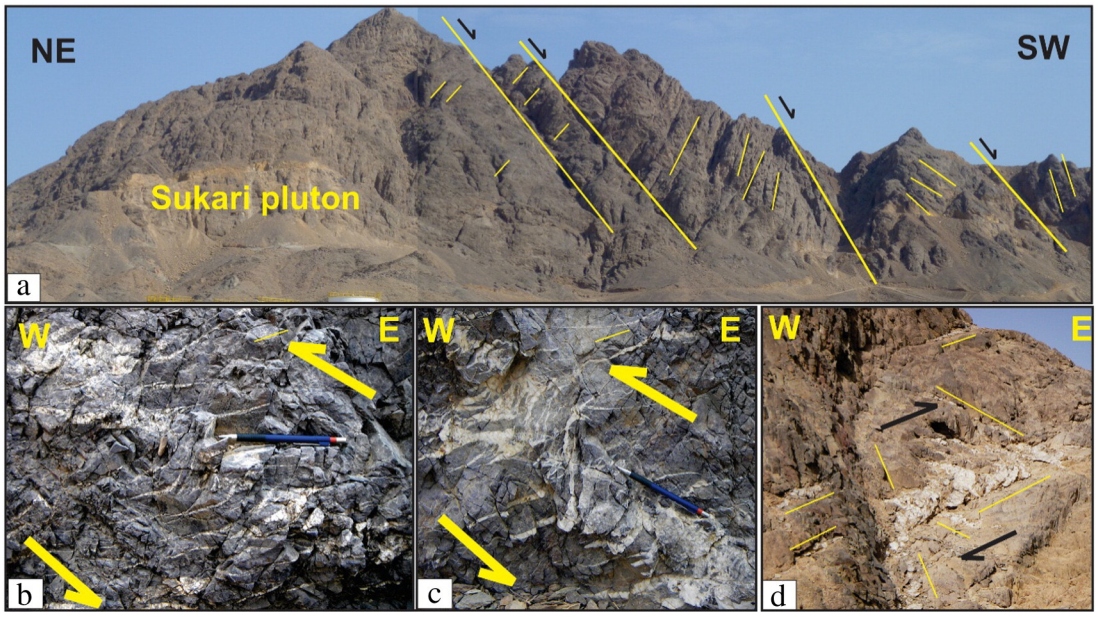

Fig. 13. (a) A series of parallel NW-trending and steeply SE-dipping step faults displaced the Sukari pluton, (b) and (c) En-echelon quartz veins in Sukari granite indicating sinistral sense of shearing, and (d) Conjugate quartz veins in Sukari granite.

Mine) trend NNE-SSW and dip toward the SSE along a series of back-thrusts that branch from the major Sukari Thrust to the west of the Sukari pluton (Fig. 10b and d).

The quartz veins are composed mainly of coarse-grained and massive quartz and are occasionally arcuate or aligned in an en-echelon arrangement (Fig. 13b-d). The lengths and thicknesses of these quartz veins vary from a few centimeters (Fig. 13d) up to more than 100 m and from a few 5 cm to 5 m, respectively. Individual composite quartz veins tend to dip more steeply (60–75°NE) than the attitude of the entire mineralized zone. The azimuthal measurement of quartz veins in the Sukari gold mine area show abundant quartz veins trending WNW-ESE (N50–70°W) and less commonly NE (N30°E) sets (Fig. 13d) with secondary trends occasionally in N-S directions (Fig. 11f and g). The quartz veins and veinlets are concentrated in the northeastern part of the Sukari pluton, where granitic rocks are highly fractured and sheared. They typically form stockworks in the northeastern part of the area. Quartz veins that trend N-S and WNW-ESE all contain gold mineralization (Fig. 11i and j). The only significant post-mineralization structures observed at Sukari to date are a set of ENE-WSW trending sub-vertical fractures associated with andesite dykes. The thickness of these dykes ranges from several centimeters to one or two meters and the fractures they fill appear to have negligible offset across them. The dykes are not always planar.

4. Kinematics

The Sukari gold mine area provides an example of a 'thin-skinned' tectonic system consisting of three structural units: the Kurdeman shear zone (KSZ), the East Sukari shear belt and the West Sukari shear zone. The KSZ is the frontal part of the major Nugrus sinistral strike-slip shear zone separating Hafafit core complex in the southwest from the Ghadir ophiolitic mélange to the northeast. Several kinematic indicators of oblique thrusting suggest that the KSZ is a transpressional imbricate zone with both thrusting and strike-slip movements. The high strain zone within the KSZ is a vertical ductile deformation zone of about 3km width and having a strike direction of N20°W. Asymmetric porphyroclasts (σ type; Hanmer and Passchier, 1991), asymmetric pressure shadows, asymmetric boudins (Goscombe and Passchier, 2003) and S/C textures observed within the high strain zone are all indicative of sinistral movement though sometimes they exhibit dextral sense of shear (Fig. 14a-g). Also, the observed kinematic indicators imply a finite reverse sinistral (i.e., oblique) slip vector on shear zones parallel to strongly plunging down-dip slip lineations, indicating WNW-side-up reverse movements.

The East Sukari shear belt consists of both thrusts and back thrusts, but it is not a simple piggyback imbricate thrust system with a unidirectional sense of thrust propagation to the southeast. The thrust system in the East Sukari shear belt is characterized by a bidirectional thrust system comprising oppositely dipping thrusts, pop-up structures and flower-like structures. The transpressive strain field is expressed most clearly around Wadi Al Alam and Wadi Um Tundubah. The strike slip shear zones are steep with a dip of 85° to S40°E. Two sets of striations are developed with southwestward plunge angles of 7° and 60° (Fig. 8e), respectively, implying that the East Sukari shear belt underwent at least two stages of sinistral strike-slip and oblique thrusting. Kinematic indicators show that both reverse and strike-slip components occurred in the East Sukari shear belt. Pop-up structure, triangle zones, and steeply NW and NE dipping foliation indicate southeast and northwest-side-up reverse movements along fore- and back-thrusts respectively. Kinematic indicators in high strain strike-slip shear zones include boudinaged (Fig. 9d), folded (Fig. 9e) and en echelon quartz veins (Fig. 9f). S/C fabrics, asymmetric deflections of foliation planes and asymmetric tails on porphyroclasts indicating sinistral sense of movement overprinted by dextral shear sense (Fig. 15a–d).

Sukari Shear zone expresses as an imbricate structure rather than a near-vertical strike-slip shear zone, consisting of several parallel thrusts and bounded by the Sukari and Um Khariga thrusts with a SE-directed movement. The Sukari Thrust has an evident imbricate fan style, which is composed of a main fault and steep branching faults in the hanging wall. The footwall of the main fault consists of volcaniclastic metasediments and basic metavolcanics in the East Sukari thrust fan with a steep dip up to 55–70° at N30–55°W and S35–65°E, whereas the hanging wall is composed mainly of volcaniclastic metasediments, schists, lenses and sheets of serpentinites. Deformation in these branch faults was very intense, resulting in strong folding in schists and volcaniclastic metasediments. A set of cleavages with a dip of 60–70° to N65°W formed in the deformed rocks, indicating southeastward thrusting of the main fault. Asymmetric tight folds in schists of the hanging wall show a southeastward vergence, indicating that these branch faults had the same thrust direction. Within the Sukari shear zone there are many vertical ductile strike-slip shear zones of about

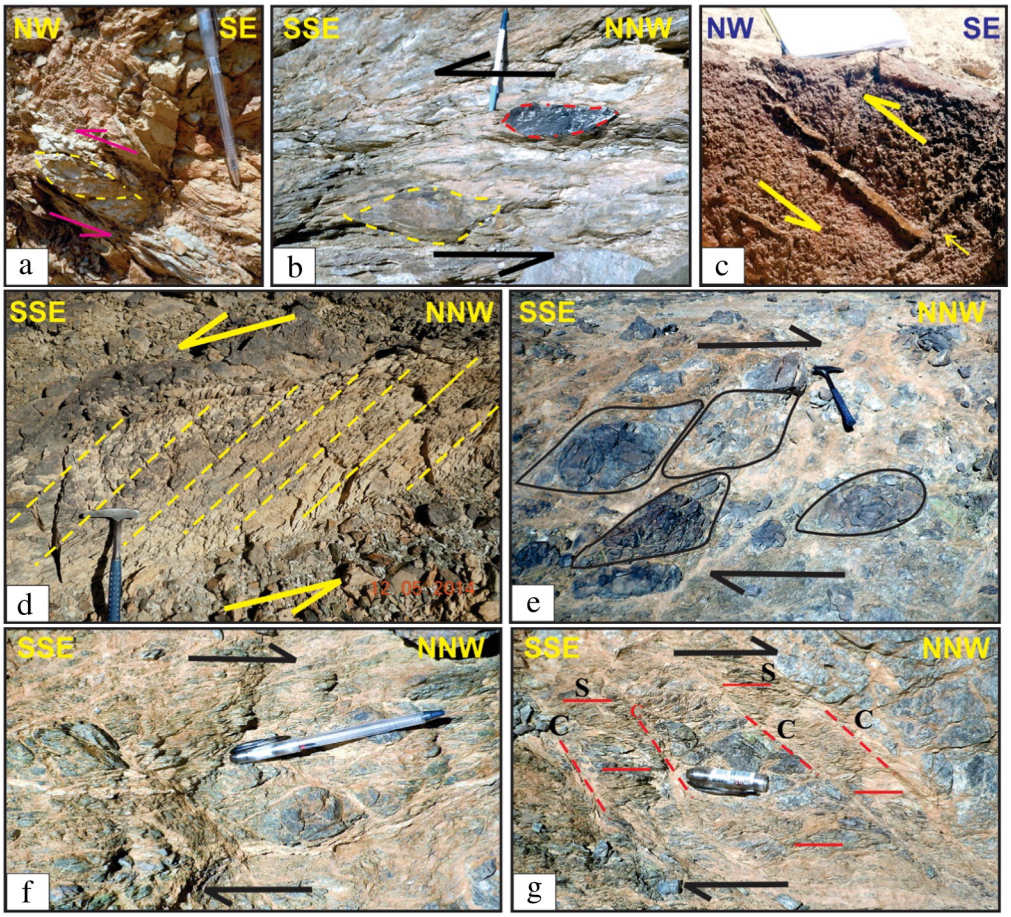

Fig. 14. Shear sense indicators from Kurdeman shear zone. Asymmetric porphyroclasts of quartz (a) and metavolcanics (b) indicating sinistral sense of shearing, (c) En echelon quartz veins showing sinistral shear sense, (d) Cleaved talc carbonate oblique to the main shear zone indicating sinistral sense of shearing, (e) and (f) Asymmetric porphyroclasts of metavolcanics indicating dextral shear sense, and (g) Shear band cleavage "c" transecting the main foliation in deformed serpentinites showing dextral shear sense.

5–20 m width and a strike direction of N30–45°E. Rocks in the deformation zone experienced intense schistosity and mylonitization, resulting in some macro-scale kinematic indicators, such as asymmetric porphyroclasts.

The C/S shear band cleavages in talc-carbonate schists were formed when S-planes traversed by C-planes parallel to the stretching lineation. The geometry of the C/S shear band cleavages, shear band boudins, pop-up structures, curvature of the shear zones and vertical folds with hinges plunging to N45°E at an angle of 75° in the highly schistose rocks indicate dextral strike-slip movement along the vertical strike-slip shear zones (Fig. 15e and f). Many of the structures indicate a component of dextral shear while less commonly they express a component of sinistral shear (e.g. Figs. 13c, d and 15g, i). However, a series of asymmetric folds parallel to the strike of the deformation zone resulted from compression perpendicular to the deformation zone, indicating thrust movement on the fault at some stage. We thus infer that the Sukari Thrust belt and the Sukari shear zone were formed in a transpressive stress field rather than a compressive one.

Small-scale thrusts, boudinaged quartz veins and pinch-and-swell structures are associated sheared granite at the western periphery of Sukari; the extension direction indicated by these structures is sub-parallel to the stretching lineation. In sheared areas within the Sukari pluton, oblique-slip shear zones with sub-vertical foliations are more common than strike slip shear zones. Deflected foliation, steep slickensides planes and quartz veins that have been folded into inclined and recumbent folds are indicative of side-up reverse movement and dextral sense of shear (Fig. 15 f and h). Some structures such as subhorizontal slickensides with variable plunges and en-echelon quartz veins indicate components of dextral and sinistral shears with dextral predominating (Fig. 15i).

5. Discussion

5.1. Deformation history

Macro- and mesoscopic structures within the Sukari gold mine area can be described in terms of three main ductile to semi-ductile deformational episodes (D_1–D_3) associated with the collision between East and West Gondwana (Stern, 2002) at ~740–540 Ma ago. D_1 is the oldest phase in the Central Eastern Desert and is simply described as an early phase of NNW-SSE shortening related to oblique island arc accretion (740–660 Ma) and characterized by NNW-directed imbrication of Pan-African nappes with the development of NNW-plunging stretching lineations and ENE-trending folds (Greiling et al., 1994). Oblique island arc accretion resulted in Pan-African nappe emplacement and the intrusion of syn-tectonic Sukari pluton at ~689 Ma. Regional nappe transport toward the NNW is common in the Eastern Desert of Egypt especially around core complexes and major shear zones (Greiling, 1997; Fritz et al., 1996; Loizenbauer et al., 2001; Abdelsalam et al., 2003; Shalaby et al., 2005; Abdeen and Abdelghaffar, 2011; Abd El-Wahed, 2008, 2014). In Sukari mine area, D_1 structures, are restricted to thrusted serpentinites sheets around Gabal Ghadir in the southeast corner of the map area. D_2 structures folded these imbricate thrusts and produced NNW-trending major upright F_2 folds in basic metavolcanics and serpentinites.

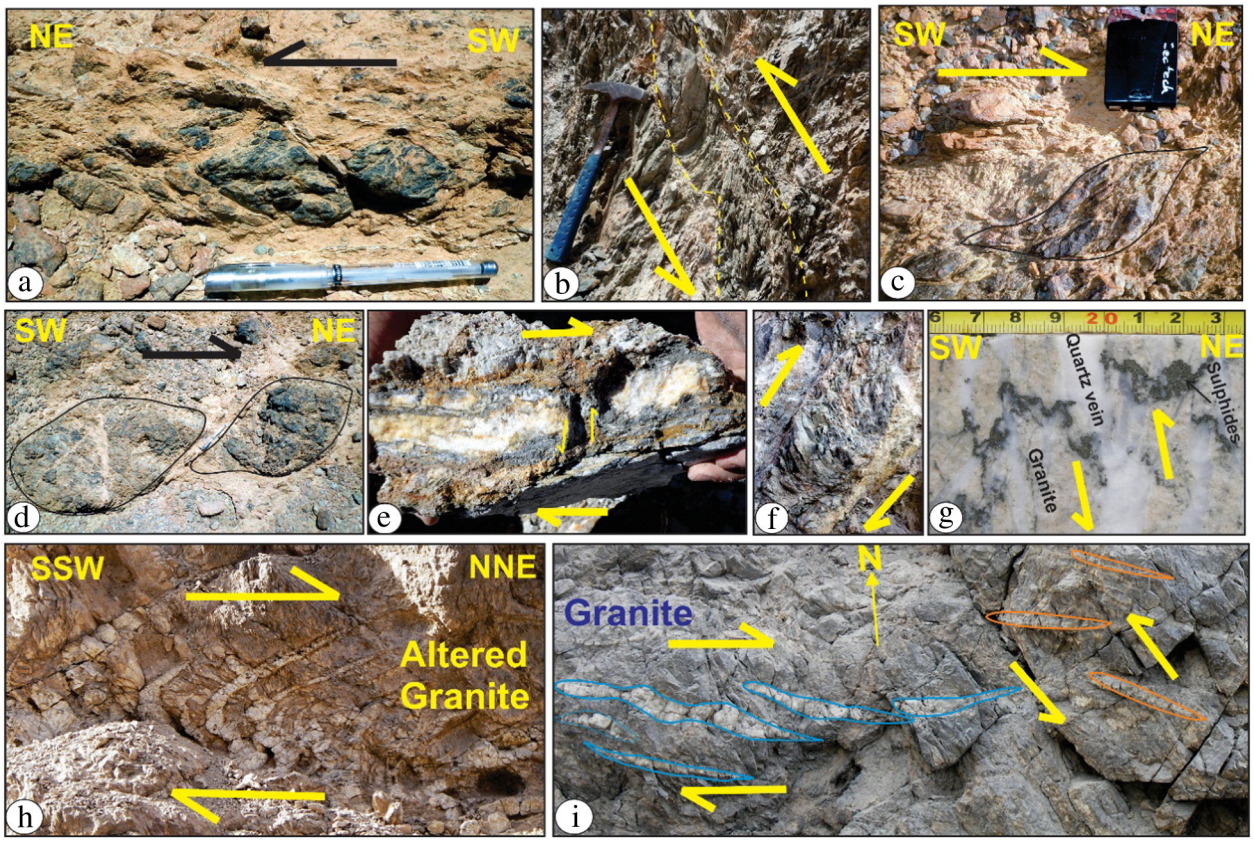

Fig. 15. Shear sense indicators from East Sukari shear belt (a–d) and Sukari shear zone (e–i): Asymmetric tails on porphyroclasts (a) and asymmetric deflections of foliation planes (b) indicating sinistral shear sense. (c) and (d) Asymmetric volcaniclastic porphyroclasts showing dextral sense of shear, (e) Displaced and deformed quartz vein showing dextral sense of shear, (f) Deflection of foliation in volcaniclastic metasediments indicate dextral shear sense, (g) Sinistrally displaced sulfidess along fracture filled with quartz vein, (h) Curved quartz veins in altered granite showing dextral sense of shear, and (i) Conjugate sets of ENE-and NNW-trending en-echelon quartz veins showing dextral and sinistral shear sense, respectively.

D_2 is associated with NW-trending sinistral strike-slip faults of the Najd Fault System (NFS), which developed at ~640–560 Ma ago. The D_2 deformation is manifested by the development of the NNW-striking KSZ, NNW-trending major F_2 with NNW-plunging axes, minor asymmetric folds of different scales (F_2), axial planar cleavage, (S_2), and crenulations (S_2), mineral stretching lineations (L_2), imbricate thrust system and steeply dipping strike–slip shear zones. Two distinct types of mineral lineations L_2 on the S_2 foliations have been recognized by measurement of minerals that grew during D_2. S_2 varies in orientation from NNW- to NE-SW and dips steeply to the NE, SW, NW and SE (Fig. 16a). The high strain within the KSZ is expressed as steeply dipping strike-slip shear zones with dominantly sub-vertical foliations and sub-horizontal lineations. In the central portions of the KSZ folds have gently plunging axes and a pervasive NW-SE striking axial planar slaty cleavage (S_2), defined by an alignment of white mica, chlorite and elongate quartz; S_2 dips 60–80° to either the SW or NE. In the eastern part of the KSZ the structures have been progressively rotated into a NE-SW orientation (arcuate zone) and transposed into the S_2 fabric in the East Sukari shear belt (Fig. 16a). Imbricate thrusts and duplex structures are commonly associated with a number of large scale asymmetrical F_2 folds. These structures, considered coeval with a consistent down-dip mineral elongation lineation, indicate a general top-to-the-northwest sense of reverse shear. Thrusting and sinistral transpression along the KSZ were synchronous with intrusion of NNW-trending mineralized major quartz veins in the Kurdeman gold mine and NE-trending veins in an arcuate thrust fan in the East Sukari shear belt, especially along Wadi Al Alam (V-shear) and Wadi Um Tundubah (Quartz Ridge).

D_2 structures formed during the NNW-trending sinistral shearing along KSZ and its arcuate thrust fan in the East Sukari thrust belt are strongly overprinted and dislocated by another imbricate fan (West Sukari thrust fan) which formed during oblique NE-trending dextral shearing (D_3) along the Sukari and Um Khariga shear zones (Fig. 16b). Tightness and steepness of major folds and curvature of the East Sukari thrust fan increases with increasing D_3 strain. D_3 deformation is manifested by the formation of the Sukari and Um Khariga thrusts, S_3 NNE-trending schistosity and crenulations, F_3 macro and small-scale folds. The outcrop-scale NE-trending F_3 folds overprint the F_2 folds in the Kurdeman gold mine area.

The quartz veins at the Kurdeman mine and in the East Sukari thrust belt were folded during NNE-dextral movement along Sukari shear zone. The undeformed NNE-trending mineralized quartz veins around the Sukari pluton developed during D_3. Lundmark et al. (2012) assigned the Sukari pluton to the first magmatic pulse (705–680 Ma) in the CED and our structural data show that the Sukari granite was magmatically active until NNE-dextral movement along Sukari shear zone and development of West Sukari thrust fan (~560 Ma).

The WNW-ESE trend of quartz veins containing gold mineralization in the Sukari pluton are related to the last phase of extensional deformation and development of NW-SE normal faults.

The geometrical relationship between D_2 major folds in the East Sukari thrust belt and the D_3 NNE-dextral shearing along Sukari shear zone indicates that the two events represent stages within a progressive deformation continuum as indicated by the termination of the D_3 NNE-trending Sukari shear zone along the inflection planes of D_2 NNW-trending KSZ. Sinistral transpression along the NW-trending shear zone in the CED (660–645 Ma) was accompanied and followed by NE-trending dextral transpression (645–540 Ma).

The latest deformation event in the Sukari mine area is related to Red Sea opening and accompanied by the generation of normal and strike-slip faults and major fractures (Fig. 3).

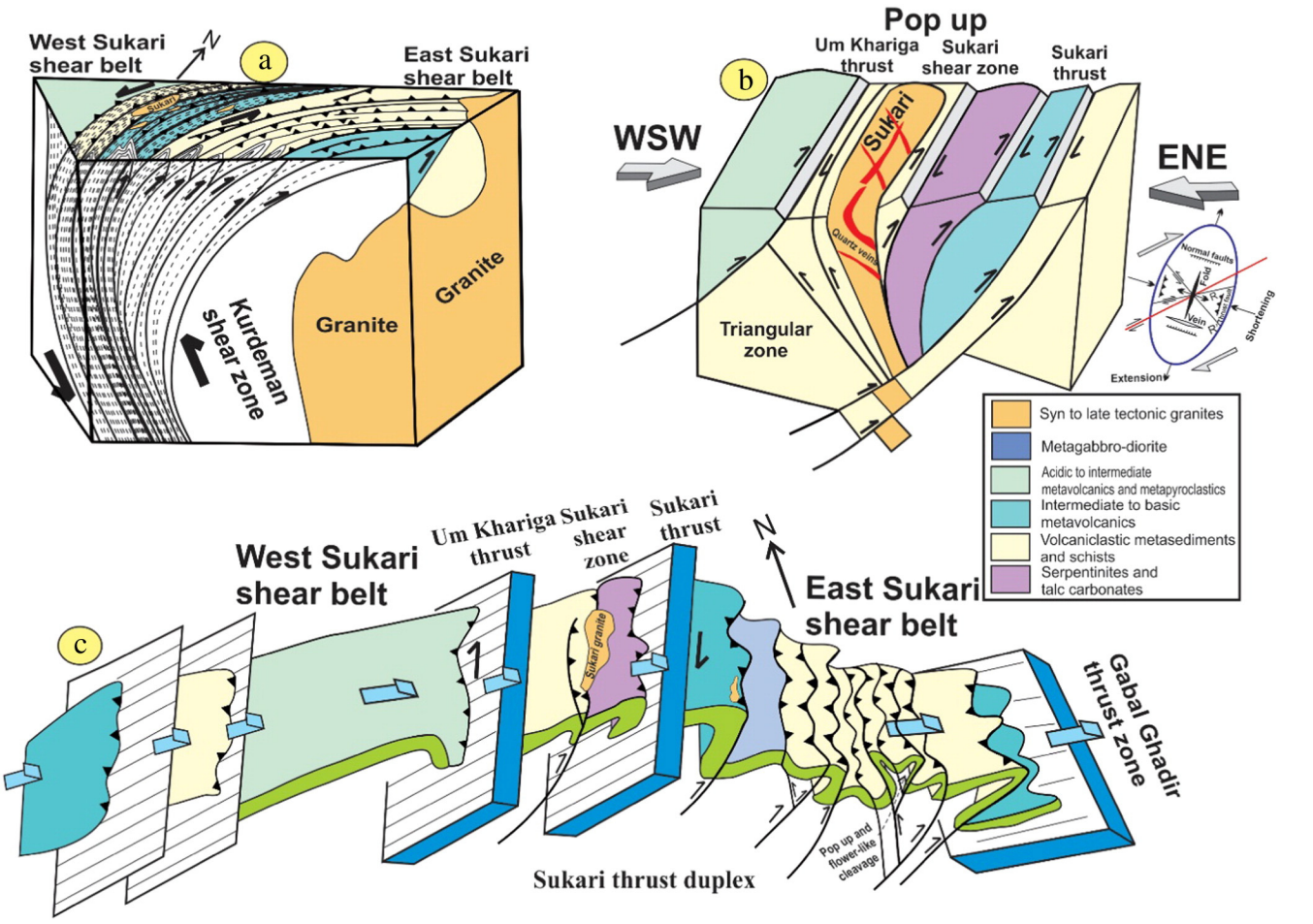

Fig. 16. (a) Geologic cross-section across Kurdeman shear zone and development of arcuate thrust fan in East Sukari shear belt, (b) A Schematic block diagram showing the geometry and kinematic of Sukari shear zone forming pop up structure suggesting transpressional tectonics, and (c) Schematic 3-D cartoon illustrating propagation of West Sukari imbricate thrust slices over the East Sukari imbricate thrust fan forming Sukari thrust duplex.

5.2. Deformation behavior

Deformation in the Sukari gold mine area reflects transpression rather than orthogonal shortening across the orogen. Transpression is considered as a wrench or transcurrent shear accompanied by horizontal shortening across, and vertical lengthening along, the shear plane (Harland, 1971; Sanderson and Marchini, 1984; King et al., 2008). Transpression is partitioned into zones of non-coaxial contraction (contraction at high angles to the shear zone boundaries with components of dip-slip simple shear and strike-slip simple shear) (Holdsworth et al., 2002; King et al., 2008). Therefore, it is likely that strike-slip and reverse faults are active at the same time during orogenic processes. NNW-sinistral and NE-dextral shear zones have played a significant role in the evolution of the Sukari arcuate-shaped structure. Both shear zones show domains that are dominated by folding, subhorizontal shortening, and a subvertical foliation.

During the initial stages of development of arcuate structure in the Sukari mine area (Fig. 16a), the NNE- and NE-trending East Sukari imbricate thrust fan branched off from the NNW-trending Kurdeman sinistral shear zone. The apparent kinematic transition from sinistral strike slip in the Kurdeman shear zone to thrusting in East Sukari shear belt superficially suggests a flower-structure configuration. Stretching lineations trending parallel to the strike of foliation, or oblique, or significantly down-dip are all possible in oblique transpression zones, so that the angle of pitch of the lineation within the foliation plane can vary from almost 0° to nearly 90° (Jones et al., 2004; Sarkarinejad and Azizi, 2008).

The structural evolution of the East Sukari thrust belt invokes a foreland-propagating deformation sequence of thrusting and folding (D_2 – D_3). East Sukari thrust belt is composed of a series of thin-thinned thrust slices characterized by two opposite thrusting directions. The early thrusts are carried in 'piggy-back' fashion on younger thrusts that develop as a result of progressive footwall collapse (Fig. 16a). The Kurdeman sinistral shear zone must root into a deep crustal low-angle detachment, marking the point at which oblique transpression is partitioned into separate strike-slip and thrust-sense shear zones in East Sukari thrust belt. The piggy-back thrust sequences propagate northwestward (foreland) while the break-back thrusts propagate southeastward (hinterland). The early thrusts are carried in 'piggyback' fashion on younger thrusts that develop as a result of progressive footwall collapse. Asymmetric porphyroclasts, and S-C fabrics indicate a consistent top-to-the-SE and sometimes NW sense of shear parallel to the mineral lineation.

Evidence that can be used to support such an evolutionary sequence includes the folding and/or breaching of early formed, high-level thrusts by younger structures in their footwalls. The origin of major tight asymmetrical folds explained by: (i) the fold-bend fault model that links fold development to movement over thrust ramps (Suppe, 1983; Sarkarinejad and Azizi, 2008; Yamamoto et al., 2007; Li et al., 2012), and (ii) the fault-propagation fold model relates fold amplification to growth and propagation of blind thrusts (Suppe, 1985; Sarkarinejad and Azizi, 2008; Alsop et al., 2010).

The East Sukari Sukari imbricates were later thrusted and overprinted by NNE-trending West Sukari imbricate thrust fan ramified

of NE-trending Mubarak-Baramiya (Fig. 2) dextral shear belt (MBSB of Abd El-Wahed and Kamh, 2010; Abd El-Wahed, 2014). The two imbricate thrust systems are characterized mainly by thrust and back-thrust forming a series of pop-up and flower-like structures (Fig. 16c). Imbricate thrust systems consist of several thrusts, each of which loses displacement upsection and eventually dies out by progressively transferring its displacement to a fold at its tip, or by distributing it among several splays (Mitra, 1986). Back-thrusts or retro-thrusts have dips and movement direction opposites to that of the main thrust (i.e. dip towards the foreland, transport towards the hinterland). The uplifted hanging-wall block between a thrust and its conjugate back-thrust forms a pop-up structure.

The Sukari Thrust has been reactivated within a transpressive shear zone where stretching lineations plunge steeply and accommodate mostly reverse motion with a component of dextral shear. Narrow zones of high strain display gently plunging lineations and accommodated mostly dextral shear with a component of reverse motion. The Sukari thrust is characterized by pop-up structures instead of the typical features of an asymmetric flower-like shape caused by southeastward thrusting. The overall contractional/dextral strike-slip nature of the West Sukari shear belt and development of the WNW-dipping Sukari Thrust and a series of ENE-dipping back-thrusts to the west of the Sukari pluton built a pop-up structure within which the Sukari pluton was uplifted (Fig. 16b and c). The small-scale steeply ENE-dipping thrusts within Sukari pluton indicate that the pluton was thrust and inverted westwards over the volcaniclastic metasediments. The tightness of major NE-trending folds in the East Sukari thrust belt is related to duplex formation and imbricate thrusting in the footwall of the West Sukari thrust belt.

Thrust-duplexes are forward foreland propagating structures formed when an imbricate thrust zone is incorporated upward into the roof fault and downward into the floor fault (Tanner, 1992; Alsop et al., 2010). Propagation of West Sukari imbricate thrust slices over the East Sukari imbricate thrust fan formed the Sukari thrust duplex. Along the Sukari Thrust, NNE-trending shear foliation, imbricated ophiolite slices and stacking form duplexes range from centimeters to meters in scale (Fig. 16c). The Sukari thrust duplex comprises the thrusts and ramps that formed the summit of Gabal Um Khariga (674 m).

The geometry and kinematics of both the Kurdeman and Sukari shear zones are consistent with general shear model or 'transpression' which involves components of both pure and simple shear (e.g. Sanderson and Marchini, 1984; Jones and Tanner, 1995; Nummer et al., 2007; Abd El-Wahed and Kamh, 2010). The formation of the high strain zones and lateral ramps are probably due to predominance of simple shear whereas, pure shear produced thrust duplexes, thrust fan and frontal ramps. Homogeneous transpression and uniform distribution of pure and simple strain (Harland, 1971) is evidenced by presence of a high-strain zone with a steeply dipping foliation and sub-horizontal stretching lineation surrounded by an imbricate thrust fan of moderately dipping thrust sheets and moderately plunging stretching lineations. The combination of strike-slip and oblique slip deformation along the Kurdeman and Sukari shear zones plus a strong component of pure shear deformation is consistent with a transpressional system (e.g. Tikoff and Teyssier, 1994; Sarkarinejad et al., 2008; Abd El-Wahed and Kamh, 2010).

The geometry and orientation of deformed and undeformed gold-bearing quartz veins suggest that they were emplaced during, at least, four mineralization phases associated with three ductile and late extensional deformation events. Deformed mineralized quartz veins consists of several moderately S-folded quartz veins and several en-echelon quartz vein arrays are oriented clockwise of the strike of the shear zones and are S-folded, suggesting sinistral and dextral shear. The deformed veins are sheared and boudinaged within the shear zones, suggesting that they formed during the development of the shear zones. The quartz vein wall are characterized by development of A "ridge-in-groove" type lineation (Lin and Williams, 1992). Because the quartz veins have a strong steeply-plunging lineation similar in orientation to the lineation in the reverse and strike-slip shear zones, the sinistral and dextral shearing of the quartz veins and steeply plunging lineation, suggest that the quartz veins were emplaced during both sinistral and dextral transpression.

The main shears and dyke swarms display a strong spatial coincidence and dyke material is commonly found in auriferous segments of the structures. The dykes may have served to focus the deformation, although the variations in the degree of deformation of the dykes suggest that they are in part syn-kinematic. The intersection and incorporation of dykes within shear zones commonly has resulted in flexuring of the shear zone and has created dilatant segments with abundant quartz veins and mineralization.

Gold mineralization at the Sukari mine area is structurally controlled by conjugate NW-sinistral and NE-dextral shear zones of the Najd Fault System as well as NW-SE extensional faults. The occureance of gold is connected with existence of granite and quartz veins. On the other hand, quartz veins are very common along the intersection between: (i) NNW- and NE-trending strike-slip shear zones, (i) Fore and back-thrusts, (iii) NW-trending normal faults and NE-trending joints (iv) Major fractures and older thrusts and shear zones. Depending on these criteria, Fig. 17a presents the recommended expected sites for gold occurrences in Sukari mine area. Some of these places have already been studied by Centamin Egypt Ltd especially Kurdeman, Sukari, Quartz Ridge, V-Shear and North Sukari. Selected Au assays from these deposits were obtained from the Centamin Company and compared with azimuth of quartz veins (Fig. 17b–f). The highest Au contents recorded at 340°–350° in Kurdeman, 40°–80° and 330°–350° in Sukari, 10°–30° in V-Shear, 60°–80° in North Sukari and 50°–70° and 320°–330° in Quartz Ridge. The highest grade of gold mineralization in Sukari such as at the Main Zone and the Hapi Zone are mainly SSE-dipping back-thrusts branching from the major Sukari Thrust and mark the western margin of Sukari granite.

5.3. Regional transpression controlling gold mineralization in the CED

Many gold-bearing quartz vein systems have formed during compressional or transpressional shearing (e.g., Bierlein and Crowe, 2000; Cox et al., 1991; Goldfarb et al., 2005; Zoheir, 2011; Zoheir and Lehmann, 2011) where the enveloping country rocks were being folded and/or reverse-faulted. Transpression involving oblique convergence has also been used to explain the geometry and kinematics of gold-bearing quartz veins in the Eastern Desert of Egypt (Hassaan et al., 2009; Zoheir, 2008, 2011; Zoheir and Lehmann, 2011; Abd El-Wahed, 2014).

Gold deposits within transpressional conjugate NW-sinistral and NE-dextral shear zones in the CED of Egypt (Fig. 1) are closely associated with granite rocks in such way that these deposits are either hosted by or occur immediately adjacent to the granite intrusions. The classification of gold-bearing quartz veins in the Eastern Desert of Egypt (Botros, 2015) classified the gold mines in the CED as follows: (i) Veins hosted in volcaniclastic metasediments and/or the syn-orogenic granites surrounding them (e.g. Sukari, Dungash, Kurdeman), (ii) Veins localized at the contacts between younger gabbros and younger granites (e.g. Atud gold mines, Harraz and Hamdy, 2015; Abdelnasser and Kumral, 2016), (iii) Quartz veins traversing calc-alkaline to mildly alkaline younger granites (e.g. Hangalia gold mine), (iv) Gold hosted in altered ophiolitic serpentinites along thrust faults (e.g. Barramiya gold mines). Gold mineralization in the Barramiya, Dungash, Sukari, Kurdeman gold mines are mainly controlled by the regional, NNW- and NE-trending zones of transpression. The Hangalia gold deposit (Khalil and Helba, 2000) and the Hamash Au–Cu deposit (Hilmy and Osman, 1989; Helmy and Kaindl, 1999) occur within post tectonic granites of Egypt. Gold mineralization at Um Rus is in quartz veins along NE-SW trending fractures in granitoid-gabbroic rocks (Harraz and El-Dahhar, 1993).

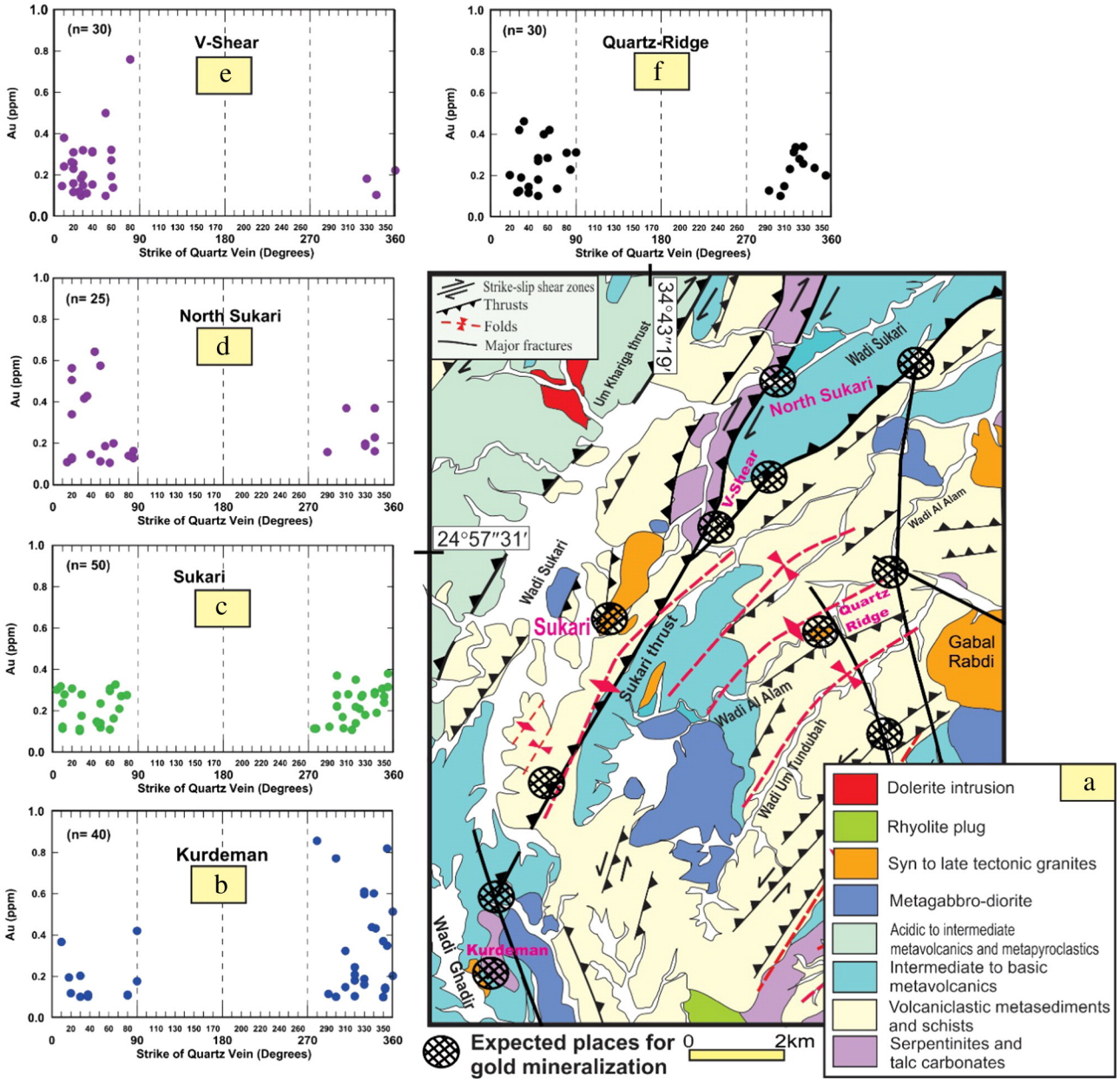

Fig. 17. (a) Expected occurrences for gold mineralization in Sukari gold mine area, and (b–f) Relations between strike of quartz veins and content of gold in some places within the Sukari mine area.

At the Barramiya gold mine (Fig. 2), the mineralized zone is represented by intensively mylonitized graphite schist, yellowish brown cavernous talc–carbonate rocks containing bodies of listwaenite and quartz veins and veinlets (Zoheir and Lehmann, 2011; Harraz et al., 2012; Botros, 2015). The Au-bearing main lode is flanked by talc–carbonate on one side and listwaenite on the other side. The mineralized and folded quartz and quartz–carbonate veins are associated with ENE-WSW dextral shear zones (Zoheir and Lehmann, 2011; Abd El-Wahed, 2014) whereas some barren and unfolded milky quartz veins are accommodated in steeply dipping NW–SE extensional fractures (Zoheir and Lehmann, 2011). The Barramiya shear belt consists of two conjugate sets of shear zones, namely a NW-SE-trending sinistral and NE-SW-trending dextral (Abd El-Wahed, 2014). Auriferous quartz and quartz-carbonate veins and altered wall-rock gouge occur where these conjugate shear zones cut through a listwaenite block adjacent to an elongate granodiorite body (Zoheir and Lehmann, 2011).

In the Dungash mine area (Fig. 2), Dungash mélange composed of remnants of imbricate ophiolitic slices tectonically intermixed with island arc metavolcanic/volcaniclastics and metasedimentary rocks. The transpressive character of deformation in the Dungash mine area is shown by the coexistence of strike-slip and dip-slip shear zones. The gold deposits at Dungash mine area occur in an EW-trending quartz vein along post-metamorphic brittle–ductile shear zones in metavolcanic and metasedimentary host rocks. Kinematic indicators along the Dungash shear zone and auriferous structures define E-W dextral shear system between foliated metavolcanic and volcaniclastic metasediments based on the sigmoidal geometry of a zone of quartz pods (Helba et al., 2001; Zoheir and Weihed, 2014; Abd El-Wahed, 2014).

The Hamash gold mine area (Fig. 2) is mainly occupied by metamudstones, phyllites, chlorite–quartz–epidote schists and actinolite–epidote schists. Serpentinite and talc–carbonate rocks are enclosed in metasediments (Hilmy and Osman, 1989; Helmy and Kaindl, 1999). Three phases of deformation were recognized in the Hamash mine area (Helmy and Kaindl, 1999): (i) D_1 is manifested by NW-trending and NE-dipping schistosity in metasediments, serpentinites, metagabbro and syn-orogenic granite. D_2 produced minor shear zones (1–2 m wide,

up to 150 m long) in metasediments and metavolcanics. These shear zones are linked with widespread hydrothermal alteration, especially in the metavolcanic rocks. D_3 produced two fault systems trending NNW-SSE and E-W defining the boundaries between the post tectonic granite and the country rocks around Hamash mine (Helmy and Kaindl, 1999). Two systems of mineralized fractures are developed in the area: one trends E-W and dips northwards, the other trends N-S and dips mainly NW. D_1 and D_2 are NW-trending and NE-trending conjugate shear zones related to the transpressional shearing of the Najd Fault System. Accordingly, the gold mineralization in Hamash mine initiated during D_2 dextral shearing and continued until D3 which an extensional phase related to intrusion of post tectonic granites.

In general, the syn-orogenic gold mineralization in the CED is connected with oblique transpression associated with conjugate NW-sinistral and NE-dextral strike slip shear zones related to the Najd fault system and hosted by volcaniclastic metasediments and altered ophiolitic serpentinites.

6. Concluding remarks

1- The Sukari mine area is within distinctive arcuate structure consisting of three structural units: the Kurdeman shear zone (KSZ), the East Sukari shear belt and the West Sukari shear zone. The KSZ is the frontal part of the Nugrus shear zone separating the Hafafit core complex in southwest from Ghadir ophiolitic mélange to the northeast.

2- The Sukari pluton is one of the oldest syn-orogenic plutons in the Central Eastern Desert and is not, as previously suggested, one of the younger granites. The Sukari pluton occurs within the hanging wall belt of Sukari Thrust with its long axes trending NNE-SSW and dipping 50–70° to the east. The geometry of the WNW-dipping Sukari Thrust and the ENE-dipping back-thrusts to the west of the Sukari pluton formed a pop-up structure along which the Sukari pluton was uplifted and displaced. The outer margins of the Sukari pluton are strongly sheared compared with its central parts. E-dipping thrusts containing deformed granites and stretched quartz veins exist in the western margin of the Sukari pluton. Gold-bearing quartz veins in Sukari granite trend mainly WNW-ESE, NE-SW and N-S.

3- The KSZ is a NNW-trending transpressional shear zone where reverse oblique slip branching arrays propagate from the KSZ forming the East Sukari NE-trending imbricate thrust fan. The East Sukari thrusts are forward-breaking or “piggy-back thrust” with southeast-side-up thrust movements (Fig. 16c).

4- The East Sukari thrust system contains all the structural features that are consistent with hinterland-dipping duplexes. The successive highly irregular thrust faults cut into the footwall forming horses and the younger thrusts tilt the previous one and the horse back toward the hinterland. These duplexes range in scale from centimeter to several hundred meters and result from intersection of NW-dipping thrusts with folded surfaces.

5- The East Sukari area is defined by a series of map-scale broad tight, high-amplitude, northeast-trending anticlines and synclines which have a general asymmetry with steep fore-limbs and back-limbs. Increasing tightening of folds is associated with intensification of cleavage and transition from upright folds to inclined and overturned folds. The thick quartz veins in the East Sukari area are nearly vertical, boudinaged, folded and their surfaces are marked by grooves and ridges parallel to the down-dip lineations.

6- The Shear sense structures indicate sinistral sense of shear in KSZ and East Sukari shear belt overprinted by dextral shearing. The Sukari shear zone shows dextral sense of shear and less common sinistral shear. Strongly plunging down-dip lineations indicate SE-side-up reverse movements.

7- The Sukari gold mine area records three deformational events. D_1 associated with NNW-propagating gently dipping thrust slices and intrusion of Sukari granite pluton. D_2 formed an arcuate-shaped structure constituting the Kurdeman shear zone (~595 Ma) and East Sukari imbricate thrust belt. D_3 is represented by the West Sukari imbricate thrust and Sukari thrust duplex. D_2 and D_3 are two stages of a single progressive deformation event with shearing along conjugate shear zones.

8- The highest Au contents in Sukari gold mine (e.g. Main Zone and Hapi Zone) are principally SSE-dipping back-thrusts branching from the major Sukari Thrust. Gold mineralization at Quartz Ridge, V-Shear and North Sukari are largely controlled by NE-trending strike-slip shear zones and transpressional imbricate thrust zones in the East Sukari Thrust belt. From the structural point of view, Quartz Ridge, North Sukari and V Shear are most suitable sites for gold exploration in Sukari mine area.

9- The NW-sinistral and NE-dextral conjugate shear zones of the Najd Fault System (620–540 Ma) and extensional NW-trending fractures play a great role in the development of gold bearing quartz veins in the Central Eastern Desert of Egypt. The sinistral and dextral transpressional imbricate thrust zones in the Sukari gold mine area are related to E-W directed shortening associated with oblique convergence between East and West Gondwana along the Mozambique belt.

Acknowledgments

The authors wish to thank Mr. Sami El-Raghy Centamin PLC for allowing us to conduct this geological work and for their hospitality during field trip to Sukari gold mine area. Thanks are due to Mr. Ismail Abdel-Khalek, Centamin's head of exploration and Mr Richard Osman, Business Development Manager at Centamin PLC for providing drill core and gold data used to construct Fig. 17. The permission to publish this data from Centamin PLC is gratefully acknowledged. In preparing this paper, use was made of company unpublished reports in the cited references. We are grateful to Professor Franco Pirajno (Editor-in-Chief) and the anonymous reviewers for their constructive comments, corrections and helpful suggestions which greatly improved the manuscript.

References

Abd El-Wahed, M.A., 2008. Thrusting and transpressional shearing in the Pan-African nappe southwest El-Sibai core complex, Central Eastern Desert, Egypt. J. Afr. Earth Sci. 50, 16–36.

Abd El-Wahed, M.A., 2010. The role of the Najd Fault System in the tectonic evolution of the Hammamat molasse sediments, Eastern Desert, Egypt. Arab. J. Geosci. 3, 1–26.

Abd El-Wahed, M.A., 2014. Oppositely dipping thrusts and transpressional imbricate zone in the Central Eastern Desert of Egypt. J. Afr. Earth Sci. 100, 42–59.

Abd El-Wahed, M.A., Kamh, S.Z., 2010. Pan-African dextral transpressive duplex and flower structure in the Central Eastern Desert of Egypt. Gondwana Research 18, 315–336.

Abdeen, M.M., Abdelghaffar, A.A., 2011. Syn- and post-accretionary structures in the Neoproterozoic Central Allaqi-Heiani suture zone, Southeastern Egypt. Precambrian Res. 185, 95–108.

Abdeen, M.M., Greiling, R.O., Sadek, M.F., Hamad, S.S., 2014. Magnetic fabrics and Pan-African structural evolution in the Najd Fault corridor in the Eastern Desert of Egypt. J. Afr. Earth Sci. 99, 93–108.

Abdelnasser, A., Kumral, M., 2016. Mineral chemistry and geochemical behavior of hydrothermal alterations associated with mafic intrusive-related Au deposits at the Atud area, Central Eastern Desert, Egypt. Ore Geol. Rev. 77, 1–24.

Abdelsalam, M.G., Abdeen, M.M., Dowaidar, H.M., Stern, R.J., Abdelghaffar, A.A., 2003. Structural evolution of the Neoproterozoic Western Allaqi–Heiani suture, southeastern Egypt. Precambrian Res. 124, 87–104.

Abdelsalam, M.G., Stern, R.J., 1996. Sutures and shear zones in the Arabian–Nubian Shield. J. Afr. Earth Sci. 23, 289–310.

Abu-Alam, T.S., Hamdy, M.M., 2014. Thermodynamic modelling of Sol Hamed serpentinite, South Eastern Desert of Egypt: implication for fluid interaction in the Arabian–Nubian Shield ophiolites. J. Afr. Earth Sci. 99, 7–23.

Akaad, M.K., Abu El Ela, A.M., El Kamshoshy, H.I., 1993. Geology of the region west of Mersa Alam, Eastern Desert, Egypt. Ann. Egypt. Geol. Surv. 19, 1–18.

Akaad, M.K., Noweir, A., 1980. Geology and Lithostratigraphy of the Arabian Desert Orogenic Belt of Egypt between Lat. 25° 35′ and 26° 30′. Bulletin of the Institute for Applied Geology King Abdulaziz University Vol. 3, pp. 127–135.

Alsop, G.I., Cheer, D.A., Strachan, R.A., Krabbendam, M.K., Kinny, P.D., Holdsworth, R.E., Leslie, A.G., Holdsworth, R.E., Krabbendam, M., Strachan, R.A., 2010. Progressive Fold and Fabric Evolution Associated with Regional Strain Gradients: A Case Study from across a Scandian Ductile Thrust Nappe, Scottish Caledonides. In: Law, R.D.,

Butler, R.W. (Eds.), Continental Tectonics and Mountain Building: The Legacy of Peach and Horne. Geological Society, London, Special Publications Vol. 335, pp. 255–274.
Andresen, A., Augland, L.E., Boghdady, G.Y., Lundmark, A.M., Elnady, O.M., Hassan, M.A., Abu El-Rus, M.A., 2010. Structural constraints on the evolution of the Meatiq Gneiss Dome (Egypt), East-African Orogen. J. Afr. Earth Sci. 57, 413–422.
Arslan, A.I., 1989. Contribution to the Geochemistry of the El Sukari Granite Pluton, Eastern Desert, Egypt. Proceedings of the. 1st Conference on Geochemistry. Alexandria University, Alexandria, Egypt, pp. 1–18.
Augland, L.E., Andresen, A., Boghdady, G.Y., 2012. U–Pb ID-TIMS dating of igneous and metaigneous rocks from the El-Sibai area: time constraints on the tectonic evolution of the Central Eastern Desert, Egypt. Int. J. Earth Sci. 101, 25–37.
Azer, M.K., 2013. Evolution and economic significance of listwaenites associated with Neoproterozoic ophiolites in South Eastern Desert, Egypt. Geol. Acta 11, 113–128.
Azzaz, A.S., 1987. Distribution of gold and associated elements in the wallrocks of the Sukkari gold deposit, Central Eastern Desert, Egypt. Arab. J. Sci. Eng. 12 (3), 243–250.
Bierlein, F.P., Crowe, D.E., 2000. Phanerozoic orogenic lode gold deposits. Rev. Econ. Geol. 13, 103–139.
Botros, N.S., 2015. The role of the granite emplacement and structural setting on the genesis of gold mineralization in Egypt. Ore Geol. Rev. 70, 173–187.
Buisson, G., Leblanc, M., 1987. Gold in mantle peridotites from Upper Proterozoic ophiolites in Arabia, Mali, and Morocco. Econ. Geol. 82, 2091–2097.
Camp, V.E., 1984. Island arcs and their role in the evolution of the western Arabian Shield. Geol. Soc. Am. Bull. 95, 913–921.
Cavaney, R.J., 2005. Geology of Sukari Gold Mine, Eastern Desert (Egypt. Internal Report to Centamin Egypt Ltd and Pharaoh Gold Mines).
Cox, S.F., Wall, V.J., Etheridge, M.A., Potter, T.F., 1991. Deformational and metamorphic processes in the formation of mesothermal vein-hosted gold deposits-examples from the Lachlan Fold Belt in Central Victoria, Australia. Ore Geol. Rev. 6, 391–423.
Dawood, Y.H., Saleh, G.M., Abd El-Naby, H.H., 2005. Effects of hydrothermal alteration on geochemical characteristics of the El Sukkari Granite, Central Eastern Desert, Egypt. Int. Geol. Rev. 47, 1316–1329.
El-Makky, A.M., Khalil, K.I., Ibrahim, I.M., 2012. Hydrothermal wall rock alteration at Kurdeman gold mine area, Eastern Desert, Egypt. Neues Jb. Mineral. Abh. 189 (1), 75–95.
Fowler, A., Osman, A.F., 2009. The Sha'it-Nugrus shear zone separating central and south eastern deserts, Egypt: a post-arc collision low-angle normal ductile shear zone. J. Afr. Earth Sci. 53, 16–32.
Fritz, H., Abdelsalam, M., Ali, K.A., Bingen, B., Collins, A.S., Fowler, A.R., Ghebreab, W., Hauzenberger, C.A., Johnson, P.R., Kusky, T.M., Macey, P., Muhongo, S., Stern, R.G., Viola, G., 2013. Orogen styles in the East African Orogen: a review of the Neoproterozoic to Cambrian tectonic evolution. J. Afr. Earth Sci. 86, 65–106.
Fritz, H., Dalmeyer, D.R., Wallbrecher, E., Loizenbauer, J., Hoinkes, G., Neumayr, P., Khudeir, A.A., 2002. Neoproterozoic tectonothermal evolution of the Central Eastern Desert, Egypt: a slow velocity tectonic process of core complex exhumation. J. Afr. Earth Sci. 34, 543–576.
Fritz, H., Wallbrecher, E., Khudier, A.A., Abu El Ela, F., Dallmeyer, R.D., 1996. Formation of Neoproterozoic metamorphic core complexes during oblique convergence, Eastern Desert, Egypt. J. Afr. Earth Sci. 23, 311–329.
Ghoneim, M.F., Bjørlykke, A., Harraz, H.Z., 1999. Rb–Sr and Sm/Nd Isotopic Systems of El Sukkari Granite, Eastern Desert, Egypt. 1st International Conference on the Geology of Africa, Assiut, Egypt, 1, pp. 281–282.
Goldfarb, R.J., Baker, T., Dube, B., Groves, D.I., Hart, C.J., Gosselin, P., 2005. Distribution, Character and Genesis of Gold Deposits Inmetamorphic Terranes. In: Hedenquist, J.W., Thompson, J.F.H., Goldfarb, R.J., Richards, J.P. (Eds.), Economic Geology 100th Anniversary Volume, pp. 407–450.
Goscombe, B., Passchier, C.W., 2003. Asymmetric boudins as shear sense indicators—an assessment from field data. J. Struct. Geol. 25, 575–589.
Greiling, R.O., Abdeen, M.M., Dardir, A.A., El Akhal, H., El Ramly, M.F., Kamal El Din, G.M., Osman, A.F., Rashwan, A.A., Rice, A.H., Sadek, M.F., 1994. A structural synthesis of the Proteorozoic Arabian–Nubian Shield in Egypt. Geol. Rundsch. 83, 484–501.
Greiling, R.O., 1997. Thrust tectonics in crystalline domains: the origin of a gneiss dome. Proc. Ind. Acad. Sci. 106, 209–220.
Greiling, R.O., Kröner, A., El-Ramly, M.F., Rashwan, A.A., El-Gaby, S., Greiling, R.O., 1988. Structural Relationships between the Southern and Central Parts of the Eastern Desert of Egypt: Details of a Fold and Thrust Belt. The Pan-African Belt of NE Africa and Adjacent Areas. Earth Evol. Sci. Vieweg, pp. 121–145.
Hanmer, S., Passchier, C., 1991. Shear Sense Indictors: A Review: Geological Survey of Canada Paper 90-17 (72 pp.).
Harland, W.B., 1971. Tectonic transpression in Caledonian Spitsbergen. Geol. Mag. 108, 27–42.
Harraz, H.Z., 1991. Lithochemical Prospecting and Genesis of Gold Deposit in the El Sukari Gold Mine, Eastern Desert, Egypt (Ph.D. thesis) Faculty of Science, Tanta University, Egypt (Bilateral Link with Oslo University, Oslo, Norway) (494pp.).
Harraz, H.Z., El-Dahhar, M.A., 1993. Nature and composition of gold-forming fluids at Umm Rus area, Eastern Desert, Egypt: evidence from fluid inclusions in vein materials. J. Afr. Earth Sci. 16, 341–353.
Harraz, H.Z., Hamdy, M.M., El-Mamoney, M.H., 2012. Multi-element association analysis of stream sediment geochemistry data for predicting gold deposits in Barramiya gold mine, Eastern Desert, Egypt. J. Afr. Earth Sci. 68, 1–14.
Harraz, H.Z., Hamdy, M.M., 2015. Zonation of primary haloes of Atud auriferous quartz vein deposit, Central Eastern Desert of Egypt: a potential exploration model targeting for hidden mesothermal gold deposits. J. Afr. Earth Sci. 101 (2015), 1–18.
Hassaan, M.M., Ramadan, T.M., Abu El Leil, I., Sakr, S.M., 2009. Lithochemical surveys for ore metals in arid region, Central Eastern Desert, Egypt: using Landsat ETM+ imagery. Aust. J. Basic Appl. Sci. 3, 512–528.
Helba, H.A., Khalil, K.I., Abdou, N.M., 2001. Alteration patterns related to hydrothermal gold mineralization in meta-andesites at Dungash area, Eastern Desert Egypt. Resour. Geol. 51, 19–30.
Helmy, H., Kaindl, R., Fritz, H., Loizenbauer, J., 2004. The Sukari Gold Mine, Eastern Desert, Egypt: structural setting, mineralogy and fluid inclusion study. Mineral. Deposita 39, 495–511.
Helmy, H.M., Kaindl, R., 1999. Mineralogy and fluid inclusion studies of the Au–Cu quartz veins in the Hamash area, South-Eastern Desert, Egypt. Mineral. Petrol. 65, 69–86.
Hilmy, M.E., Osman, A., 1989. Remobilization of gold from a chalcopyrite–pyrite mineralization Hamash gold mine, Southeastern Desert, Egypt. Mineral. Deposita 24, 244–249.
Holdsworth, R.E., Tavarnelli, E., Clegg, P., Pinheiro, R.V.L., Jones, R.R., McCaffrey, K.J.W., 2002. Domainal deformation patterns and strain partitioning during transpression: an example from the southern uplands terrane, Scotland. J. Geol. Soc. Lond. 159, 401–415.
Johnson, P.R., Andresen, A., Collins, A.S., Fowler, A.R., Fritz, H.W., Ghebreab, W., Kusky, T., Stern, R.J., 2011. Late Cryogenian–Ediacaran history of the Arabian–Nubian Shield: a review of depositional, plutonic, structural, and tectonic events in the closing stages of the northern East African Orogen. J. Afr. Earth Sci. 61, 167–232.
Jones, R.R., Tanner, P.W.G., 1995. Strain partitioning in transpression zones. J. Struct. Geol. 17, 793–802.
Jones, R.R., Holdsworth, R.E., Clegg, P., McCaffrey, K., Travarnelli, E., 2004. Inclined transpression. J. Struct. Geol. 30, 1531–1548.
Khalil, K.I., Helba, A., 2000. Gold mineralization and its alteration zones at the Hangalia Gold Mine area, Eastern Desert, Egypt. Egypt. Mineral. 12, 65–92.
King, D.S., Klepeis, K.A., Goldstein, A.G., Gehrels, G.E., Clark, G.L., 2008. The initiation and evolution of the transpressional Straight River shear zone, central Fiordland, New Zealand. J. Struct. Geol. 30, 410–430.
Li, P., Zhang, J., Guo, L., Yang, X., 2012. Structural features and deformational ages of the northern Dabashan thrust belt. Geosci. Fornt. 3, 41–49.
Lin, S., Williams, P.F., 1992. The origin of ridge-in-groove slickenside striae and associated steps in an S-C mylonite. J. Struct. Geol. 14, 315–321.
Loizenbauer, J., Wallbrecher, E., Fritz, H., Neumayr, P., Khudeir, A.A., Kloetzil, U., 2001. Structural geology, single zircon ages and fluid inclusion studies of theMeatiq metamorphic core complex: implications for Neoproterozoic tectonicsin the Eastern Desert of Egypt. Precambr. Res. 110, 357–383.
Lundmark, A.M., Andresen, A., Hassan, M., Augland, L.E., Boghdady, G.Y., 2012. Repeated magmatic pulses in the East African Orogen in the Eastern Desert, Egypt: an old idea supported by new evidence. Gondwana Res. 22, 227–237.
McClay, K.R. (Ed.), 1992. Thrust Tectonics. Chapman and Hall, London (457pp).
Meert, J.G., 2003. A synopsis of events related to the assembly of eastern Gondwana. Tectonophysics 362, 1–40.
Mitra, S., 1986. Duplex structures and imbricate thrust systems: geometry, structural position and hydrocarbon potential. Bull. Am. Assoc. Pet. Geol. 70, 1087–1112.
Nummer, A.R., Machado, R., Dehler, N.M., 2007. Pluton emplacement in a releasing bend in a transpressive regime: the arrozal granite in the Paraba do Sul shear belt, Rio de Janeiro. Ann. Braz. Acad. Sci. 79 (2), 299–305.
Rice, A.H.N., Osman, A.F., Abdeen, M.M., Sadek, M.F., Ragab, A.I., 1993. Preliminary Comparison of six Late-to Post-Pan-African Molasse Basins, E. Desert, Egypt. In: Thorweihe, U., Schandelmeier, H. (Eds.), Geoscientific Research in Northeast AfricaProceedings of the International Conference on Geoscientific Research in Northeast Africa. Balkema, Rotterdam, pp. 41–45.
Sanderson, D.J., Marchini, W.R.D., 1984. Transpression. J. Struct. Geol. 6, 449–457.
Sarkarinejad, K., Faghih, A., Grasemann, B., 2008. Transpressional deformations within the Sanandaj–Sirjan metamorphic belt (Zagros Mountains, Iran). J. Struct. Geol. 30, 818–826.
Sarkarinejad, K., Azizi, A., 2008. Slip partitioning and inclined dextral transpression along the Zagros Thrust System, Iran. J. Struct. Geol. 30, 116–136.
Shalaby, A., Stüwe, K., Makroum, F., Fritz, H., Kebede, T., Klotzli, U., 2005. The Wadi Mubarak belt, Eastern Desert of Egypt: a Neoproterozoic conjugate shear system in the Arabian–Nubian Shield. Precambrian Res. 136, 27–50.
Sharara, N.A., 1999. Stable Isotopes and Fluid Inclusions of the Gold Mineralizations at El Sukkari District, Central Eastern Desert, Egypt: Genetic Constraints. International Conference on Geochemistry, Alexandria University, Egypt, 15–16 Sept 1999, pp. 317–339.
Sharara, N.A., Vennemann, T.W., 1999. Composition and Origin of the Fluid Responsible for Gold Mineralization in some Occurrences in the Eastern Desert, Egypt: Evidence from Fluid Inclusions and Stable Isotopes. Proceedings of the 1st International Conference on the Geology of Africa, Assiut, Egypt, 1, pp. 421–445.
Smith, P., Osman, R., Franzmann, D., Johnson, N., Boreham, C., 2014. Mineral Resource and Reserve Estimate for the Sukari Gold Project. Egypt. Internal Technical Report, Centamin Egypt Ltd (177p.).
Stern, R.J., 1985. The Najd fault system, Saudi Arabia and Egypt: a Late Precambrian rift-related transform system. Tectonics 4, 497–511.
Stern, R.J., 1994. Arc assembly and continental collision in the Neoproterozoic East African Orogen implications for the consolidation of Gondwanaland. Annu. Rev. Earth Planet. Sci. 22, 319–351.
Stern, R.J., 2002. Crustal evolution in the East African Orogen: a neodymium isotopic perspective. J. Afr. Earth Sci. 34, 109–117.
Stern, R.J., Johanson, P.R., Kröner, A., Yibas, B., 2004. Neoproterozoic Ophiolites of the Arabian–Nubian Shield. In: Kusky, T.M. (Ed.), Precambrian Ophiolites and Related RocksDevelopments in Precambrian Geology Vol. 13. Elsevier, Amsterdam, pp. 95–128.
Suppe, J., 1983. Geometry and kinematics of fault bend folding. Am. J. Sci. 283, 684–721.
Suppe, J., 1985. Principles of Structural Geology. Prentice-Hall, Englewood Cliffs, NJ (537 pp.).

Talavera, C., 2013. Zircon SHRIMP Geochronology of Samples from Sukkari Porphyry (Egypt). Unpublished Report for Greg Hall, 12pp.
Tanner, P.W., 1992. Morphology and geometry of duplexes formed during flexural-slip folding. J. Struct. Geol. 14 (10), 1173–1192.
Tikoff, B., Teyssier, C., 1994. Strain modeling of displacement-field partitioning in transpressional orogens. J. Struct. Geol. 16, 1575–1588.
Unzog, W., Kurz, W., 2000. Progressive development of lattice preferred orientations (LPOs) of naturally deformed quartz within a transpressional collision zone (Panafrican orogen in the Eastern Desert of Egypt). J. Struct. Geol. 22, 1827–1835.
Yamamoto, H., Yamamoto, S., Kaneko, Y., Terabayashi, M., Komiya, T., Katayama, I., Iizuka, T., 2007. Imbricate structure of the Luobusa Ophiolite and surrounding rock units, southern Tibet. J. Asian Earth Sci. 29, 296–304.
Zoheir, B.A., 2008. Characteristics and genesis of shear zone-related gold mineralization in Egypt: a case study from the Um El Tuyor mine, south Eastern Desert. Ore Geol. Rev. 34, 445–470.
Zoheir, B.A., 2011. Transpressional zones in ophiolitic mélange terranes: potential exploration targets for gold in the South Eastern Desert, Egypt. J. Geochem. Explor. 111, 23–38.
Zoheir, B.A., Lehmann, B., 2011. Listvenite-lode association at the Barramiya gold mine, Eastern Desert, Egypt. Ore Geol. Rev. 39, 101–115.
Zoheir, B.A., Weihed, P., 2014. Greenstone-hosted lode-gold mineralization at Dungash mine, Eastern Desert, Egypt. J. Afr. Earth Sci. 99 (1), 165–187.